Ocean warming combined with lower omega-3 nutritional availability impairs the cardio-respiratory function of a marine fish

Marie Vagner, Eric Pante, Amelia Viricel, Thomas Lacoue-Labarthe, Jose-Luis Zambonino-Infante, Patrick Quazuguel, Emmanuel Dubillot, Valerie Huet, Herve Le Delliou, Christel Lefrançois, et al.

© 2019. Published by The Company of Biologists Ltd | Journal of Experimental Biology (2019) 222, jeb187179. doi:10.1242/jeb.187179

RESEARCH ARTICLE

Ocean warming combined with lower omega-3 nutritional availability impairs the cardio-respiratory function of a marine fish

Marie Vagner[1,*,§], Eric Pante[1], Amelia Viricel[1], Thomas Lacoue-Labarthe[1], Jose-Luis Zambonino-Infante[2], Patrick Quazuguel[2], Emmanuel Dubillot[1], Valerie Huet[1], Herve Le Delliou[2], Christel Lefrançois[1,‡] and Nathalie Imbert-Auvray[1,‡]

ABSTRACT

Highly unsaturated fatty acids of the omega-3 series (HUFA) are major constituents of cell membranes, yet are poorly synthesised *de novo* by consumers. Their production, mainly supported by aquatic microalgae, has been decreasing with global change. The consequences of such reductions may be profound for ectotherm consumers, as temperature tightly regulates the HUFA content in cell membranes, maintaining their functionality. Integrating individual, tissue and molecular approaches, we examined the consequences of the combined effects of temperature and HUFA depletion on the key cardio-respiratory functions of the golden grey mullet, an ectotherm grazer of high ecological importance. For 4 months, fish were exposed to two contrasting HUFA diets [4.8% eicosapentaenoic acid (EPA)+docosahexaenoic acid (DHA) on dry matter (DM) versus 0.2% EPA+DHA on DM] at 12 and 20°C. Ventricular force development coupled with gene expression profiles measured on cardiac muscle suggest that combining HUFA depletion with warmer temperatures leads to: (1) a proliferation of sarcolemmal and sarcoplasmic reticulum Ca^{2+} channels and (2) a higher force-generating ability by increasing extracellular Ca^{2+} influx via sarcolemmal channels when the heart has to sustain excessive effort due to stress and/or exercise. At the individual scale, these responses were associated with a greater aerobic scope, maximum metabolic rate and net cost of locomotion, suggesting the higher energy cost of this strategy. This impaired cardiac performance could have wider consequences for other physiological performance such as growth, reproduction or migration, all of which greatly depend on heart function.

KEY WORDS: Omega-3 highly unsaturated fatty acids, Temperature, Cardiac performance, Swimming performance, *Chelon auratus*, RNAseq

INTRODUCTION

The highly unsaturated fatty acids of the *n*-3 series (also called long-chain omega-3 HUFA, and simply HUFA through this paper) are critical structural and functional components of the cell membranes of most animal tissues, making them vitally important for numerous key physiological functions in aquatic and terrestrial organisms. HUFA are, however, weakly synthesised *de novo* by animals, and must be obtained through food (Glencross, 2009; Tocher, 2010). In natural food webs, they are mainly supplied by marine microalgae (Crawford and Broadhurst, 2012; Pahl et al., 2010). This HUFA production, sitting at the base of aquatic food webs, determines HUFA availability for the upper trophic levels, as the fatty acid (FA) content in the tissues of animals is a reflection of their diet (Arts et al., 2001; Crawford and Broadhurst, 2012; Gladyshev et al., 2009). In marine fish, membranous HUFA are mainly represented by ecosapentaenoic acid (EPA, 20:5n-3) and docosahexaenoic acid (DHA, 22:6n-3; Glencross, 2009; Tocher, 2010), mostly supplied by diatoms. Fish constitute one of the main vectors of HUFA from aquatic ecosystems to human populations (Arts et al., 2001).

Global change, through warming, acidification or hypoxia, is leading to the lowered production of HUFA at the base of food webs, due to the alteration of the FA biosynthesis pathways and species assemblages of microalgae (Galloway and Winder, 2015; Hixson and Arts, 2016). Reductions of 8.2% for EPA and 27.8% for DHA are expected as a consequence of a temperature increase of 2.5°C (Hixson and Arts, 2016). This lowered HUFA production may decrease the HUFA availability for higher trophic levels (Gladyshev et al., 2009, 2011; Kang, 2011). For example, a 1°C increase in sea surface temperature in the SW Pacific Ocean is expected to decrease EPA and DHA content in tuna by 3% and 1.5%, respectively, as a result of a decreasing biomass of HUFA-rich diatoms in favour of HUFA-poor dinoflagellates (Pethybridge et al., 2015). Although a few studies have described the ability of marine fish to stimulate, at the molecular level, the FA desaturation pathways in response to a HUFA dietary depletion, this process has never been shown to compensate for HUFA depletion in tissues (Glencross, 2009; Sargent et al., 1997; Tocher, 2010; Vagner et al., 2007, 2009).

Such changes in the HUFA composition of consumers may have cascading detrimental effects throughout the world's ecosystems, affecting the physiology of many species, and consequently their role within ecosystems, and culminating in an overall decline in the global availability of these nutrients for human health (Arts et al., 2001; Gladyshev et al., 2009; Hixson and Arts, 2016). Despite this, the various consequences of changing HUFA availability remain largely understudied.

Previous studies have reported that the degree of lipid unsaturation in cell membranes is correlated with the activity of membrane-bound enzymes and rates of transmembrane proton leakage, with consequences for enzyme activities and whole-animal metabolism (Hulbert and Else, 2000; Kraffe et al., 2007; Martin et al., 2012). For example, Wagner et al. (2004) suggested that a low dietary HUFA/saturated FA ratio caused a decline in Atlantic salmon swimming performance tested at 10–12°C; however, the

[1]UMR 7266 LIENSs (University of La Rochelle – CNRS), 2 rue Olympe de Gouges, 17000 La Rochelle, France. [2]Ifremer, UMR 6539 LEMAR, Center Ifremer ZI Pointe du diable, 29280 Plouzané, France.
*Present address: CNRS, UMR 6539 LEMAR, Center Ifremer ZI Pointe du diable, 29280 Plouzané, France.
‡These authors contributed equally to this work

§Author for correspondence (marie.vagner@univ-brest.fr)

M.V., 0000-0002-2777-006X; E.P., 0000-0001-7680-2112; A.V., 0000-0002-2789-6869; T.L.-L., 0000-0002-4682-8730; J.-L.Z.-I., 0000-0001-8436-4773; P.Q., 0000-0003-3503-2347; V.H., 0000-0003-0976-5600; H.L.D., 0000-0001-7909-3817; C.L., 0000-0001-6904-1722; N.I.-A., 0000-0003-0445-335X

Received 19 June 2018; Accepted 20 December 2018

Journal of Experimental Biology (2019) 222, jeb187179. doi:10.1242/jeb.187179

opposite relationship was found in Atlantic salmon exposed to 9°C (McKenzie et al., 1998). These contrasting results for the same species suggested potential interactions between HUFA food content and acclimation temperature on fish physiology. This interaction was recently demonstrated in a species highly tolerant to temperature variations, the golden grey mullet, *Chelon auratus*: the detrimental effects of a low HUFA diet were greater in warmer conditions (20°C versus 12°C), resulting in greater energy expenditure to reach a given swimming speed (Vagner et al., 2015). Highlighting these combined effects is of particular importance given the strong seasonal temperature variations that occur in temperate coastal areas, and the predicted scenario of a 3°C increase in ocean water temperature by 2100 (IPCC, 2013).

The underlying mechanisms governing the metabolic response observed by Vagner et al. (2015) have never been explored, but they are key to further understanding and predicting fish responses to the nutritional and thermal challenges induced under climate change. In the present study, we hypothesised that temperature and HUFA food content affect fish metabolism through a modulation of cardiac function, which is key to supplying the required amount of oxygen and nutrients to tissues (Claireaux, 2005; Clark et al., 2005). HUFA depletion in cardiomyocyte membranes combined with a warmer environment could modify the conformation of the ionic pumps and channels embedded in cell membranes (Raynard and Cossins, 1991; Turner et al., 2003), with consequences for the cardiomyocyte contraction capacity. This contraction is normally initiated after depolarisation of the cell, and graded by an increase in the concentration of free intracellular calcium (Ca^{2+}), supplied through: (1) an external Ca^{2+} influx across the sarcolemma, via either L-type Ca^{2+} channels or a Na^{+}/Ca^{2+} exchanger, and (2) internal Ca^{2+} mobilisation from storage in the sarcoplasmic reticulum (SR). In fish, Ca^{2+} influx derives mainly from L-type Ca^{2+} channel activity (Chatelier et al., 2006; Driedzic and Gesser, 1994; Vornanen, Shiels and Farrell, 2002). Relaxation is then rapidly regulated by a decrease in free cytoplasmic Ca^{2+} largely governed via the Na^{+}/Ca^{2+} exchanger (in reverse mode), but also via Ca^{2+}-ATPase pumps (SERCA), and sometimes via sarcolemmal (SL) Ca^{2+}-ATPase pumps (PMCA).

In this context, this study evaluates the cardiac response of fish as a first step towards understanding the combined effects of environmental temperature and lowering HUFA food content, by integrating responses at molecular (gene expression), tissue (cardiac performance) and individual (oxygen consumption during swimming effort) levels. This work aims to improve our understanding of the integrative response of fish to environmental changes, which is a challenge burdened with ecological and socio-economic consequences, as well as public health concerns.

MATERIALS AND METHODS

We used golden grey mullets, *Chelon auratus* (Risso 1810), from the same experimental groups as those used by Vagner et al. (2015): they were exposed to two highly contrasting HUFA diets (a high and a low HUFA diet), chosen according to the needs defined for several fish species, and two contrasting environmental acclimation temperatures that are representative, respectively, of mean winter (12°C) and mean summer (20°C) temperatures in the Pertuis Charentais area (Rochebonne, France). Their cardio-respiratory performance was then measured at the individual level in terms of metabolic rates and associated swimming effort. The physiological mechanisms underlying this response were studied: (1) on isolated hearts in order to evaluate cardiac performance in terms of contraction and relaxation capacity and the relative involvement of SL channels and/or exchangers and the SR in excitation–contraction coupling, and (2) at the transcriptional level to evaluate differences in gene expression in heart tissue according to the experimental conditions tested.

Ethics statement

All fish manipulations were performed according to the Animal Care Committee of France (ACCF). No specific permissions were required from the Departmental Service of Fisheries to collect *C. auratus* in their natural environment, as this is not a protected or endangered species, and as a relatively small number of fish were collected for this research (n=160 individuals) compared with their abundance in this fishing area. The protocol was approved by the ACCF (approval number: 17-300-2). All fish manipulations were performed under anaesthesia (tricaine methane sulphonate MS-222; 0.1 g l^{-1}, Sigma-Aldrich, St Quentin-Fallavier, France), and all efforts were made to minimise suffering.

Fish maintenance

Juvenile golden grey mullets (initial mean±s.e.m. mass: 6.1±0.2 g; initial mean±s.e.m. standard length: 7.0±0.1 cm) were caught in the marine coastal area of La Rochelle (France) in 2012 and transported in an aerated tank to the laboratory, where all experiments were conducted. Upon arrival, fish were transferred into four indoor tanks (volume: 400 l; n=40 fish per tank) that were individually supplied with aerated recirculated sand-filtered natural seawater and equipped with an external biological filter (Eheim professional 3 2080, Eheim, Deizisau, Germany). Fish were progressively acclimated to the water tank temperature, which was kept constant by a recirculating water system (TECO TR20, Conselice, Italy), and maintained in a temperature-controlled room (20°C) exposed to a 12 h light:12 h dark photoperiod cycle. Temperature (18.7±0.04°C), salinity (29.3±0.5) and oxygen (87.9±2.6% air saturation) were monitored daily using a conductimeter (WTW model Oxi 340i, Weildeim, Germany). After a few days of acclimation to the experimental structure, each of the four initial tanks was separated in two tanks (n=8 tanks of 400 l each with n=20 fish per tank), and water temperature was progressively modified to reach 12°C (mimicking winter temperature in a temperate coastal area: 12.5±0.1°C; n=4 tanks) or 20°C (mimicking summer temperature in a temperate coastal area: 19.8±0.1°C; n=4 tanks). Fish were initially fed with a commercial diet (Le Gouessant® aquaculture, Lamballe, France) once a day for 1 month.

They were then progressively fed with two experimental isolipidic and isoproteic diets differing in their HUFA content (the experimental diet to commercial diet ratio was increased every 2 days from 25%:75% to 50%:50%, 75%:25% and finally to 100%:0%). The two experimental diets were formulated and made at the Ifremer-PFOM unit, UMR 6539 LEMAR (Plouzané, France): a high HUFA diet (HH: 4.8% EPA+DHA on a dry matter basis), and a low HUFA diet (LH: 0.2% EPA+DHA on a dry matter basis). The LH diet was obtained by replacing the fish oil present in the HH diet with soybean oil. Diets were formulated taking a standard diet as the reference (1.2% EPA+DHA on a dry matter basis), as previously formulated for the same species (Vagner et al., 2014). The composition and FA content of the two experimental HH and LH diets are summarised in Vagner et al. (2015). For each of these two diets, the fish in two tanks per experimental temperature were fed for at least 4 months (2% of biomass per day) to ensure a good incorporation of dietary lipids into their cell membranes (Vagner et al., 2007, 2014, 2015). The four experimental conditions were created in duplicate and called HH20, LH20, HH12 and LH12.

Journal of Experimental Biology (2019) 222, jeb187179. doi:10.1242/jeb.187179

Growth

Just before being exposed to the two experimental LH and HH diets (T0), all fish were starved for 24 h and anaesthetised (MS-222; 0.1 g l^{-1}, Sigma-Aldrich), weighed and pit-tagged (MS-120; biolog-id, Réseaumatique, Bernay, France). Each month, the fish were anaesthetised under the same conditions and individually identified using a pit-tag reader before fresh mass (±0.1 g), total length, standard length (i.e. notochord length), height and width (±0.01 cm) were measured. The thermal-unit growth coefficient (TGC) was used rather than specific growth rate in order to take into account the temperature, and was calculated as shown in Eqn 1 (Iwama and Tautz, 1981):

$$\mathrm{TGC} = \frac{({m_{\mathrm{final}}}^{1/3} - {m_{\mathrm{initial}}}^{1/3})}{(T \times D)} \times 1000, \quad (1)$$

where m is fish body mass, T is the acclimation temperature (i.e. 12 or 20°C) and D is the number of acclimation days before fish were tested in the swim-tunnel respirometer (i.e. 98 days for the 20°C group or 182 days for the 12°C group).

Metabolic performance

Fish swimming and metabolic performance were assessed using a swim-tunnel respirometer (Loligo Systems, Tjele, Denmark) in June 2013 for the 20°C-acclimated individuals (i.e. after 4 months of exposure to the experimental diet) and in September 2013 for the 12°C-acclimated individuals (i.e. after 7 months of exposure to the experimental diet). This lag allowed the fish to at least double their body mass from the beginning of the feeding period, ensuring an accurate oxygen consumption signal detection in the swim-tunnel respirometer.

Swim-tunnel respirometer experimental setup

The experimental setup of the swim-tunnel respirometer was the same as described in Vagner et al. (2014, 2015). Briefly, the respirometer (volume: 10 l) was composed of: (i) a swim chamber with a square working section (40 cm length, 10 cm height, 10 cm width) and (ii) a hydraulic system placed upstream to promote a laminar flow in the swim chamber. No correction was made for the solid blocking effects of the fish in the working section, as the calculated fractional error was <5% of the working section area (Webb, 1975). The flow in the respirometer was generated by an electric motor with a propeller. It was calibrated before the start of experiments and the speed ranged between 0 and 150 cm s^{-1}. A flush pump allowed water exchange between the respirometer and the external bath, in which water temperature and oxygenation were controlled. Temperature was kept constant (12 or 20°C) by a recirculating water system from the external bath (TECO TR20).

Oxygen consumption measurements

Oxygen concentration in the respirometer was continuously measured with an oxygen probe (PreSens GmbH, Regensburg, Germany) connected to an oximeter (Oxy-4, PreSens GmbH), transferring data every 10 s to a storage computer. The oxygen concentration was automatically adjusted according to the real-time temperature recorded in the respirometer. Oxygen consumption rate ($\dot{M}_{O_2}$) was measured by intermittent-flow respirometry, based on an alternation between (i) a flushing phase (5 min) and (ii) a measuring phase (20 min), during which the flush pump was turned off, preventing the inflow of water from the external bath into the respirometer. The $\dot{M}_{O_2}$ (mg O_2 kg^{-1} h^{-1}) was calculated as shown in Eqn 2 (Lefrancois and Claireaux, 2003; Vagner et al., 2008):

$$\dot{M}_{O_2,\mathrm{meas}} = \left(\frac{\Delta\,[O_2]}{\Delta t}\right) \times \left(\frac{V}{m}\right), \quad (2)$$

where $\Delta[O_2]$ is the oxygen concentration decrease (mg O_2 l^{-1}) relative to the fish oxygen consumption with respect to time Δt (h), V is the swim-tunnel water volume (10 l) minus the volume of the fish, and m is fish mass (kg).

$[O_2]$ versus time was plotted, and for each $\dot{M}_{O_2}$ measurement, a linear regression was adjusted (Graphical Analysis 3.4, Beaverton, OR, USA). This allowed the determination of $\Delta[O_2]/\Delta t$ and a regression coefficient illustrating $\dot{M}_{O_2}$ measurement accuracy. Only those measurements with a regression coefficient above 0.9 were considered. The bacterial $\dot{M}_{O_2}$ was measured for half an hour before and after each experiment, and the mean of both was subtracted from the $\dot{M}_{O_2}$ measured.

As respiratory metabolism depends on animal mass, $\dot{M}_{O_2}$ was standardised for a 100 g fish, as in Eqn 3 (Schurmann and Steffensen, 1994; Vagner et al., 2008):

$$\dot{M}_{O_2,\mathrm{corr}} = \dot{M}_{O_2,\mathrm{meas}} \times \left(\frac{m_{\mathrm{meas}}}{m_{\mathrm{corr}}}\right)^{1-A}, \quad (3)$$

where $\dot{M}_{O_2,\mathrm{corr}}$ (mg O_2 kg^{-1} h^{-1}) is the oxygen consumption for a corrected mass (m_{corr}=100 g), $\dot{M}_{O_2,\mathrm{meas}}$ is the measured $\dot{M}_{O_2}$ (mg O_2 kg^{-1} h^{-1}), m_{meas} is the measured fish mass (kg) and A is the allometric exponent describing the relationship between metabolic rate and fish mass. A has never been determined for *C. auratus*. We therefore used a value of 0.8, which was estimated in different teleost species (Schurmann and Steffensen, 1994), and has previously been employed for *C. auratus* (Vagner et al., 2014, 2015).

Critical swimming speed (U_{crit}) test

Fish starved for 96 h (HH20 group: mean±s.e.m. mass: 36.7±0.6 g, standard length: 12.72±0.3 cm, n=14; LH20 group: 33.1±2.4 g, 12.3±0.3 cm, n=13; HH12 group: 11.6±0.6 g, 8.9±0.2 cm, n=14; LH12 group: 12.3±0.8 g, 8.9±0.2 cm, n=12) were randomly sampled in tanks using a net, and individually tested in the swim-tunnel respirometer at their acclimation temperature. Fish were subjected to a step-protocol based on progressive swimming speed increments following the protocol fully described in Vagner et al. (2014). At each swimming step, the velocity was maintained for 20 min and $\dot{M}_{O_2}$ was measured. Oxygen saturation never fell below 75% of air saturation during $\dot{M}_{O_2}$ measurements. The water in the respirometer was renewed through a flush pump during the swimming speed increment phase (i.e. between two consecutive swimming steps). This allowed the oxygen saturation to return to >85% of air saturation. The speed increments were repeated until fish exhaustion. Fish were considered to be exhausted when: (1) they were maximally laterally bent on the grid placed at the rear of the swim chamber, forming a C-shape, or (2) they were unable to swim away from this grid for more than 10 s of stimulation through the tunnel window at the rear of the swim chamber. The stimulation involved lighting (with a 150 W spotlight) the rear part of the chamber, which created a high contrast with the shadow area at the front.

Fish sampling after U_{crit} test

At the end of the U_{crit} test, speed was progressively decreased to 0.5 body lengths (BL) s^{-1} and fish were anaesthetised (MS-222; 0.1 g l^{-1}), identified using a pit-tag reader, weighed (±0.1 g, and

Journal of Experimental Biology (2019) 222, jeb187179. doi:10.1242/jeb.187179

measured (±0.1 cm). Fish body condition was evaluated using the Fulton index (FI) as in Eqn 4 (Fulton, 1904):

$$\mathrm{FI} = \frac{m}{L^3}, \quad (4)$$

where m is fish mass in g and L is total fish length in cm.

Blood was sampled (1 ml) by caudal puncture using chilled heparinised syringes. All manipulations were performed quickly so that blood was obtained within 2–3 min of transfer into the anaesthetic solution. Haematocrit (percentage of red blood cells in the centrifuged blood volume) was measured immediately in duplicate in capillary tubes centrifuged for 3 min at 8000 ***g*** at 4°C. Fish were dissected on ice (4°C) to collect the liver and heart for assessment of the hepatosomatic index (HSI) and cardiosomatic index (CSI) using Eqns 5 and 6:

$$\mathrm{HSI} = \frac{(m_{\mathrm{liver}} \times 100)}{(m_{\mathrm{fish}} - m_{\mathrm{liver}})}, \quad (5)$$

$$\mathrm{CSI} = \frac{(m_{\mathrm{heart}} \times 100)}{(m_{\mathrm{fish}} - m_{\mathrm{heart}})}, \quad (6)$$

where m_{liver} is liver mass, m_{heart} is heart mass and m_{fish} is fish mass.

Muscle was collected for lipid analysis above the lateral line in the caudal part of the fish (Martinez, 2003). It was immediately frozen in liquid nitrogen and stored at −80°C for further lipid analysis. The heart was stored in liquid nitrogen before being transferred to a −80°C freezer for storage pending transcriptomic analyses.

Determination of U_{crit}, metabolic rates and aerobic scope

The following parameters were calculated for each fish: U_{crit}, standard metabolic rate (SMR), active metabolic rate (MMR), aerobic scope (AS) and net cost of transport (NCOT) per unit distance.

U_{crit} (in BL s^{-1}) was calculated using Eqn 7 (Brett, 1964):

$$U_{\mathrm{crit}} = U_t + \frac{t_1}{t} \times U_1, \quad (7)$$

where U_t (BL s^{-1}) is the highest velocity maintained for an entire swimming step, t_1 (min) is the amount of time spent at the fatigue velocity, t (min) is the prescribed swimming period (20 min) and U_1 is the last increment velocity (1.5 or 0.75 BL s^{-1}).

SMR (mg O_2 kg^{-1} h^{-1}) was extrapolated as the intercept (i.e. $\dot{M}_{O_2}$ when swimming velocity U=0 BL s^{-1}; Brett, 1964) of Eqn 8:

$$\dot{M}_{O_2} = \mathrm{SMR}\, e^{bU}, \quad (8)$$

where $\dot{M}_{O_2}$ is oxygen consumption (mg O_2 kg^{-1} h^{-1}), b is a constant and U is swimming speed (BL s^{-1}).

MMR (mg O_2 kg^{-1} h^{-1}) was considered as the highest $\dot{M}_{O_2}$ recorded during the U_{crit} test.

AS (mg O_2 kg^{-1} h^{-1}) was determined for each fish as the difference between MMR and SMR, and represents the aerobic scope of the individual to perform its energy-demanding activities (Brett, 1964).

NCOT (mg O_2 kg^{-1} m^{-1}) to reach U_{crit} was calculated for each fish according to Clark et al. (2011) as in Eqn 9:

$$\mathrm{NCOT} = \frac{(\mathrm{MMR} - \mathrm{SMR})}{U_{\mathrm{crit}}}. \quad (9)$$

Lipid analysis

The lipid analysis methodology and the resulting data used in the present study were first reported in Vagner et al. (2015). Briefly, lipid analysis was performed on fish muscle at the beginning (n=10 fish as control; t_0) and after the period of exposure to the experimental diet (n=13 fish per experimental condition). Total lipid was extracted and fractionated into neutral (lipids of reserves) and polar lipids (lipids in membranes). FA analyses were performed on both of these lipid classes by gas chromatography. The muscle tissue was chosen because it is involved in anaerobic/aerobic metabolism during swimming performance. It was always taken on the right side, above the lateral line and below the spinal column, just behind the operculum. For technical reasons, FA analysis was not performed on cardiac tissue (the amount of tissue was not sufficient to perform both lipid and transcriptomic analyses), but numerous mammalian and fish studies have established that the HUFA composition of cardiac membrane phospholipids is directly influenced by dietary fat intake, and similar levels of HUFA were measured in muscle and hearts (Bell et al., 1993; Bell et al., 1991; Lopez-Jimena et al., 2015; Owen et al., 2004; Thomassen and Røsjø, 1989). The results of individual FA composition are expressed as a percentage of total identified fatty acid methyl esters (FAME).

Chemical analyses of the experimental diets were performed in duplicate for each sample and both the method and the resulting data are also reported in Vagner et al. (2015).

Ventricular tissue contractility

Another set of 24 h-starved fish (HH20 group: mean±s.e.m. mass: 49.3±2.2 g, standard length: 13.9±0.2 cm, n=15; LH20 group: 50.3±2.6 g, 14.1±0.2 cm, n=17; HH12 group: 14.3±0.7 g, 9.4±0.2 cm, n=20; LH12 group: 14.4±1.1 g, 9.4±0.3 cm, n=7) were randomly sampled in September 2013 (i.e. after 7 months of exposure to the experimental diet) in tanks using a net, and individually anaesthetised (MS-222; 0.1 g l^{-1}). The preparation of cardiac tissue for measuring isometric tension and adrenergic sensitivity was as detailed in Shiels and Farrell (1997). Briefly, the heart was rapidly excised and placed in physiological saline (pH 7.8 with Tris base). For each heart (HH20 group: mean±s.e.m. heart mass: 41.8±2.3 mg; LH20 group: 45.0±1.9 mg; HH12 group: 20.8±1.0 mg; LH12 group: 21.4±1.3 mg), two 1 mm-wide ventricular strips were dissected out and tied at either end with a spring and stretched. Four strips (i.e. n=2 per fish) were tested simultaneously. Each strip was lowered into a water-jacketed organ bath containing 20 ml of oxygenated physiological saline thermoregulated at 20 or 12°C (Ministat, Huber, Edison, NJ, USA) corresponding to the temperature at which hearts of the 20°C- and 12°C-acclimated fish were tested, respectively. They were stretched until the tension reached a peak and were then allowed to equilibrate for 30 min under basal stimulation (0.2 Hz). Strips were then subjected to the protocols described below, during which they were triggered using a stimulator and two flattened platinum electrodes. Signals from the isometric force transducer (MLT0201/184, ADInstruments, Dunedin, New Zealand) were amplified (Power Lab, ADInstruments) and displayed on a chart recorder (LabChart 7 pro, ADInstruments).

Adrenergic sensitivity

Adrenaline solution (10 µmol l^{-1}, Sigma-Aldrich) was used to investigate the adrenergic sensitivity of ventricular tissue. As a β-type adrenergic receptor agonist, adrenaline increased the density of the L-type calcium current by elevating the open-probability of the L-type calcium channels (Hove-Madsen, 1992; Vornanen, 1996,

1998) after phosphorylation (Shiels et al., 1998). This increases the force of contraction. Adrenaline also stimulates the Ca^{2+}-ATPase pump of the SR, accelerating relaxation. As adrenaline is naturally present at nanomolar concentrations in resting fish (Gamperl, 2004), a low adrenaline concentration (10 nmol l^{-1}) was used as the control for the subsequent tests on (1) the effects of maximal adrenergic solution (10 µmol l^{-1} adrenaline) and (2) the effects of ryanodine (see below). The adrenaline doses used in this study (10 nmol l^{-1} and 10 µmol l^{-1}) were, respectively, the minimum and maximum values of the dose–response curve (Keen et al., 1994). Under conditions of increased energetic demand, such as stress, the adrenaline concentration in circulation can indeed reach 10 µmol l^{-1} (Mc Donald and Milligan, 1992). The control solution of adrenaline (10 nmol l^{-1}) was added to each of the four baths. After a 10 min equilibration period, the four ventricular strips were exposed to the force–frequency trials where the pacing frequency was successively 0.2 (i.e. 12 beats min^{-1}), 0.5, 0.8, 1, 1.6 and 2 Hz (i.e. 120 beats min^{-1}). At the end of the trials, the frequency was returned to the basal level of 0.2 Hz. The adrenergic sensitivity was then evaluated by adding a saline physiological solution containing adrenaline (10 µmol l^{-1}) to two of the four ventricle strips. The two other strips were used as controls, by adding the tonic concentration of adrenaline (10 nmol l^{-1}) in order to account for muscle fatigue when adrenaline (10 µmol l^{-1}) was added (Shiels and Farrell, 2000). After a 10 min equilibration period, the strips were exposed to the different stimulation frequencies listed above (from 0.2 to 2 Hz).

Participation of the SR

To test the relative contribution of the SR to the isometric contraction of the ventricle, 10 µmol l^{-1} of ryanodine (Shiels and Farrell, 1997) was added to each of the four baths containing the two ventricular strips pre-treated either with the tonic control adrenaline solution (10 nmol l^{-1}) or with 10 µmol l^{-1} adrenaline. After a 30 min period of stabilisation, the strips were exposed to successive increasing stimulations from 0.2 to 2 Hz. During the stabilisation period, ryanodine is assumed to be bound irreversibly to the Ca^{2+} channel on the SR (Rousseau et al., 1987), rendering it ineffective and unable to contribute to force development.

Data analyses

The data were analysed using the software LabChart 7 pro (ADInstruments). The contraction rate (mN mm^{-2} min^{-1}), half-relaxation rate (mN mm^{-2} min^{-1}), time to peak tension (min) and peak tension (mN mm^{-2}) were calculated at each pacing frequency. Pumping capacity (mN mm^{-2} min^{-1}), the product of peak tension and heart frequency responses, served as an index of the heart power output (Matikainen and Vornanen, 1992).

Transcriptomic analysis of cardiac tissue

RNA extraction and library construction

Total RNA was isolated from heart tissues stored at −80°C (see 'Fish sampling after U_{crit} test', above) using the RNeasy Plus Mini Kit (Qiagen, Hilden, Germany) containing a genomic DNA eliminator solution, following the manufacturer's protocol. To obtain enough RNA for library preparation, at least 10 µg of heart tissue from two to three individuals exposed to the same experimental condition were pooled. A total of five RNA extracts (sample replicates) per experimental condition (LH20, LH12, HH20, HH12) were obtained. RNA integrity was estimated using an Agilent 2100 Bioanalyzer with Agilent RNA 6000 nanochips and reagents (Agilent Technologies, Les Ulis, France). RNA integrity number ranged from 6.6 to 8.7 (mean±s.d. 7.65±0.6), indicating the high and consistent quality of RNA samples. RNA concentration was measured using a NanoDrop ND-1000 spectrophotometer (Wilmington, DE, USA).

Libraries were constructed at the Dyneco lab (Ifremer, Plouzané, France) based on 500 ng of total RNA and using the TruSeq stranded RNA kit (Illumina®, San Diego, CA, USA) with reagent quantities adapted by Dr M. Le Gac (Dyneco) from the GeT-PlaGe (Toulouse, France) based on Illumina (Illumina®) protocols. mRNA was isolated, and the poly-A tails purified using poly-T oligo-attached magnetic beads via two rounds of purification. During the second elution of the poly-A mRNA, the mRNA was fragmented and primed for cDNA synthesis. The cleaved mRNA fragments were then copied into first-strand cDNA using reverse transcriptase and random hexamer primers. This step was followed by second-strand cDNA synthesis, which removed the RNA template and synthesised a replacement strand, incorporating dUTP in place of dTTP to generate double-strand cDNA. The incorporation of dUTP quenches the second strand during amplification, because the polymerase does not incorporate past this nucleotide. AMPure XP beads were used to separate the double-strand cDNA from the second strand reaction mix. At the end of the process, the cDNA was blunt-ended. Then, for each sample, a unique mRNA simple adapter index was ligated at the end of the cDNA fragments. The libraries obtained were then amplified by PCR performed on a Peqstar Peqlab thermocycler (Peqlab Biotechnologie GmbH, Erlangen, Germany) with a PCR primer cocktail that anneals to the ends of the adapters, and using the following protocol: 98°C for 30 s; 16 cycles of 98°C for 10 s, 60°C for 30 s, 72°C for 30 s; 72°C for 5 min. The number of cycles was minimised to avoid skewing the representation of the library. After cleaning of PCR products, library quality was assessed on an Agilent 2100 Bioanalyzer using Agilent high-sensitivity DNA analysis chips and reagents (Agilent Technologies). Libraries were quantified using the Kapa Library Quantification Kit (Kapa Biosystems, Wilmington, MA, USA) with ROX Low qPCR master mix, on a QuantStudio 3 thermocycler (Applied Biosystems, Foster city, CA, USA) according to the manufacturer's instructions: 95°C for 5 min, 35 cycles of 95°C for 30 s, 60°C for 45 s.

The 20-indexed cDNA libraries (mean±s.d. insert length 280.9±38 bp, range 240–373 bp) were normalised at 3 nmol l^{-1} and pooled in equal volume (5 µl) before being sent for sequencing (2×150 bp) on one Illumina HiSeq3000 lane at the GeT-PlaGe France Genomics Sequencing Platform (Toulouse, France).

Bioinformatic treatment of transcriptomic data

Read quality was assessed using FastQC v.0.11.5 after each step of the pipeline until assembly. Raw data were trimmed using Trimmomatic v.0.36 (Bolger et al., 2014) and de-duplicated (exact duplicate reads were removed) using the Dedupe function within Geneious v.10.1.3 (Kearse et al., 2012) on the default settings. Reads were filtered using Deconseq v.0.4.3 (Schmieder and Edwards, 2011) to remove potential contaminant sequences from rRNA of eukaryotes, viruses, bacteria and archaea (SILVA database; Quast et al., 2012) and from human transcripts (Deconseq database). The *de novo* transcriptome assembly was performed with Trinity v.2.4.0 (Grabherr et al., 2011) on the default settings.

Assembly quality was evaluated using four criteria (as recommended in Honaas et al., 2016): (1) the proportion of reads mapping back to the assembly (determined using Bowtie v. 2.1.0; Langmead and Salzberg, 2012), (2) the recovery of genes conserved

across eukaryotes, vertebrates and Actinopterygii (assessed using BUSCO v.3; Simão et al., 2015; Waterhouse et al., 2018), (3) the contig length distribution (N50) and (4) the number of genes. The assembly statistics are provided in Table S1.

TransDecoder (Haas et al., 2013) was used to detect putative coding regions within transcripts (open reading frames ≥100 amino acids long). Homology to known proteins was determined using blastp and pfam searches following the pipeline provided on the TransDecoder website (https://github.com/TransDecoder/TransDecoder/wiki). Transcripts were functionally annotated using Trinotate within Trinity. Transcript quantification was performed on the trimmed reads, followed by an analysis of differential gene expression among the four experimental conditions using Salmon (Patro et al., 2017) within Trinity. Finally, we used gene ontology (GO) terms to describe gene functions and their interactions (Gene Ontology Consortium, 2004). We performed a GO term enrichment analysis using GOseq (Young et al., 2010) as implemented in Trinity. In this analysis, we used the GO terms assigned to differentially expressed transcripts in order to test whether specific biological processes, cellular components or molecular functions (Gene Ontology Consortium, 2004) were over-represented among these differentially expressed transcripts. For example, the biological process 'regulation of ion transmembrane transport' (Table 1) is found to be 'enriched' if this process is statistically over-represented among the annotated differentially expressed transcripts (which can be under- or over-expressed). We used REVIGO (Supek et al., 2011) to reduce the functional redundancy between these GO sets and summarise the functional response to temperature and HUFA concentration in the diet. The analysis pipeline is shown in Fig. S1.

Statistical analysis

Data are presented as means±s.e.m. All statistical analyses were performed with R v.3.3.1 (2016). The level of significance for statistical analyses was always set at α=0.05.

Slopes of growth regression curves were determined for each fish. The effects of diet and temperature on these slopes, as well as on TGC, U_{crit}, SMR, MMR, AS, NCOT, haematocrit, HSI, CSI and FI, were tested using a two-way ANOVA (Table 2). The fish muscle/food content FA ratio was calculated for DHA, EPA and two of their precursors, i.e. the stearidonic acid 18:4n-3 and the alpha-linolenic acid 18:3n-3. The effects of diet and temperature on these ratios were also tested using a two-way ANOVA. When two-way ANOVA indicated significant interactions between diet and temperature, the differences between means were compared using a Tukey HSD test. Prior to ANOVA analyses, homoscedasticity was tested using Levene's test. Normality was tested on the residuals using the Shapiro test.

The effects of acclimation temperature, food, stimulation frequency and their interactions on cardiac variables (i.e.

Table 1. List of GO terms associated with regulation of ion transmembrane transport (GO:0034765) by REVIGO

Term ID	Description	Frequency	$\log_{10}$FDR	Uniqueness	Dispensability
GO:0034765	Regulation of ion transmembrane transport	0.197%	−7.1412	0.53	0.00
GO:1901019	Regulation of calcium ion transmembrane transporter activity	0.011%	−7.1412	0.54	0.88
GO:2000021	Regulation of ion homeostasis	0.043%	−2.9226	0.71	0.76
GO:1901021	Positive regulation of calcium ion transmembrane transporter activity	0.004%	−2.9466	0.54	0.93
GO:0032507	Maintenance of protein location in cell	0.057%	−2.3006	0.62	0.90
GO:1903169	Regulation of calcium ion transmembrane transport	0.020%	−6.7462	0.55	0.84
GO:2001259	Positive regulation of cation channel activity	0.006%	−1.8606	0.54	0.95
GO:2001258	Negative regulation of cation channel activity	0.005%	−1.7580	0.56	0.84
GO:0010959	Regulation of metal ion transport	0.069%	−6.5090	0.56	0.89
GO:2001257	Regulation of cation channel activity	0.020%	−5.4919	0.54	0.96
GO:0034762	Regulation of transmembrane transport	0.202%	−6.8359	0.56	0.84
GO:0051279	Regulation of release of sequestered calcium ion into cytosol	0.012%	−2.8220	0.45	0.94
GO:0051270	Regulation of cellular component movement	0.169%	−1.5674	0.52	0.78
GO:0010881	Regulation of cardiac muscle contraction by regulation of the release of sequestered calcium ion	0.001%	−4.7939	0.28	0.94
GO:0010880	Regulation of release of sequestered calcium ion into cytosol by sarcoplasmic reticulum	0.003%	−5.2879	0.48	0.75
GO:0022898	Regulation of transmembrane transporter activity	0.036%	−6.2923	0.55	0.99
GO:0051049	Regulation of transport	0.529%	−2.1953	0.55	0.87
GO:0032412	Regulation of ion transmembrane transporter activity	0.035%	−6.2491	0.54	0.93
GO:0032409	Regulation of transporter activity	0.039%	−6.0698	0.59	0.74
GO:0032414	Positive regulation of ion transmembrane transporter activity	0.012%	−4.0559	0.54	0.93
GO:1901379	Regulation of potassium ion transmembrane transport	0.014%	−2.6398	0.52	0.89
GO:0010522	Regulation of calcium ion transport into cytosol	0.019%	−2.6117	0.47	0.91
GO:1901381	Positive regulation of potassium ion transmembrane transport	0.005%	−1.9050	0.52	0.93
GO:1901385	Regulation of voltage-gated calcium channel activity	0.003%	−2.8112	0.56	0.82
GO:0043271	Negative regulation of ion transport	0.022%	−2.7391	0.57	0.82
GO:0043270	Positive regulation of ion transport	0.040%	−2.7436	0.55	0.85
GO:0043269	Regulation of ion transport	0.244%	−6.5841	0.55	0.85
GO:0043268	Positive regulation of potassium ion transport	0.006%	−1.9955	0.56	0.94
GO:0043266	Regulation of potassium ion transport	0.017%	−3.0493	0.57	0.85
GO:1901896	Positive regulation of calcium-transporting ATPase activity	0.000%	−1.4049	0.57	0.75
GO:1901894	Regulation of calcium-transporting ATPase activity	0.001%	−1.3463	0.58	0.84
GO:0051924	Regulation of calcium ion transport	0.043%	−5.2879	0.55	0.89
GO:0051651	Maintenance of location in cell	0.059%	−2.8246	0.62	0.75
GO:0045185	Maintenance of protein location	0.067%	−1.9955	0.66	0.90

$\log_{10}$FDR refers to the GO enrichment test performed by GOseq.

Table 2. Swimming, metabolic and condition indices measured for each experimental group

Group	U_{crit} (BL s^{-1})	SMR (mg O_2 kg^{-1} h^{-1})	MMR (mg O_2 kg^{-1} h^{-1})	AS (mg O_2 kg^{-1} h^{-1})	Hct (%)	NCOT (mg O_2 kg^{-1} m^{-1})	FI	TGC (g deg day^{-1})	HSI	CSI
HH20	8.8±0.4 (*n*=14)	20.1±2.2^{a} (*n*=16)	211.6±10.0^{b} (*n*=14)	191.2±10.4^{b} (*n*=14)	48.5±2.9 (*n*=17)	22.4±1.4^{b} (*n*=13)	1.11^{E-2}±1^{E-3b} (*n*=18)	3.8^{E-1}±2.2^{E-1b} (*n*=34)	1.6±0.1^{a} (*n*=17)	0.11±0.01^{a} (*n*=16)
LH20	9.1±0.3 (*n*=13)	23.6±3.0^{a} (*n*=12)	234.9±7.2^{c} (*n*=13)	213.8±6.3^{c} (*n*=12)	41.1±2.9 (*n*=13)	23.9±1.0^{b} (*n*=13)	1.10^{E-2}±3^{E-4b} (*n*=14)	3.4^{E-1}±0.4^{E-1b} (*n*=20)	1.2±0.1^{a} (*n*=14)	0.10±0.00^{a} (*n*=13)
HH12	9.6±0.3 (*n*=14)	37.4±4.1^{b} (*n*=12)	57.8±13.1^{a} (*n*=10)	128.6±13.8^{a} (*n*=11)	38.2±1.6 (*n*=9)	12.9±1.5^{a} (*n*=11)	0.95^{E-2}±2^{E-4a} (*n*=14)	0.8^{E-1}±0.3^{E-1a} (*n*=37)	1.7±0.1^{b} (*n*=14)	0.12±0.01^{b} (*n*=14)
LH12	9.1±0.3 (*n*=12)	27.9±3.9^{b} (*n*=12)	135.5±10.7^{a} (*n*=11)	100.5±9.5^{a} (*n*=10)	34.9±1.2 (*n*=10)	12.0±1.5^{a} (*n*=10)	1.00^{E-2}±2^{E-4a} (*n*=11)	0.8^{E-1}±0.3^{E-1a} (*n*=17)	1.7±0.1^{b} (*n*=9)	0.12±0.01^{b} (*n*=8)
Statistics	NS	Temp**	Food×Temp* Temp***	Food×Temp* Temp***	Food* Temp**	Temp***	Temp***	Temp***	Temp*	Temp*

Fish were fed with LH (low HUFA food content) or HH (high HUFA food content) diet and acclimated at winter-like (12°C, fish tested in September 2013 in 12°C seawater) or summer-like (20°C, fish tested in June 2013 in 20°C seawater) temperatures. Data are critical swimming speed (U_{crit}; BL, body lengths), standard metabolic rate (SMR), maximum metabolic rate (MMR), aerobic scope (AS), haematocrit (Hct, % of red blood cells), net cost of transport (NCOT), Fulton index (FI), thermal-unit growth coefficient (TGC), hepatosomatic index (HSI) and cardiosomatic index (CSI). Data are presented as means±s.e.m. and the number (*n*) of statistical samples is indicated. Asterisks indicate the level of significance (*P<0.05, **P<0.01, ***P<0.001). NS, no significant effect; Temp, temperature; Food×Temp, interactive effect between temperature and food. See Results for further statistical details (P, F, d.f.$_1$ and d.f.$_2$ values). In the MMR and AS columns, values not sharing a common letter are significantly different.

contraction rate, peak tension, pumping capacity, relaxation rate) were measured with the idea of comparing overall trends in heart tissue function in each experimental group. They were tested by applying linear mixed-effects models. Individual identity was considered as a random factor in order to take into account the repeated exposure of the heart of each individual to the successive frequencies and chemical stimulations. All models were computed using the *lmer* fitting routine in R (lme4 package; R Core Team 2013).

The pumping capacity curve was fitted using a polynomial model for each individual to determine the stimulation frequency at which optimum pumping capacity occurs. These frequency values were then compared between groups using non-parametric Wilcoxon tests.

RESULTS

FA composition in fish

The FA composition in fish muscle from the four experimental groups (HH20, LH20, HH12 and LH12) is fully presented in Vagner et al. (2015). Briefly, and as expected, the final fish FA composition reflected that of the diet, and HH fish presented a higher HUFA content than LH fish. In addition, EPA content was significantly affected by an interaction between diet and temperature, and was significantly less incorporated in LH20 fish.

The fish muscle/food content ratios for 18:3n-3, 18:4n-3, DHA and EPA are presented in Fig. 1. Values of this ratio above 1 suggest the selective incorporation or synthesis of this FA in fish tissue, to cope with potential deficiencies. Values around or below 1 suggest that the FA does not need to be retained, because its supply from food is close to the fish's physiological needs. Here, the 18:3n-3 ratio was below 1 for all experimental groups, suggesting that the supply of this FA from both diets corresponded to the needs of all groups, independently of their acclimation temperature. This FA ratio was significantly affected by temperature (ANOVA: $F_{1,46}$=17.11, P=1.48×10^{-4}), diet (ANOVA: $F_{1,46}$=4.54, P=3.80×10^{-2}) and an interaction between the two factors (ANOVA: $F_{1,46}$=6.43, P=0.01; Fig. 1), and was significantly highest for the HH12 group. This indicates the better incorporation of this FA in this group.

The 18:4n-3 and EPA ratios were also significantly affected by temperature (ANOVA 18:4n-3: $F_{1,46}$=49.68, P=7.71×10^{-9}; EPA: $F_{1,46}$=8.36, P=5.8×10^{-3}), diet (ANOVA 18:4n-3: $F_{1,46}$=125.49, P=9.75×10^{-15}; EPA: $F_{1,46}$=160.47, P=2×10^{-16}) and the interaction between the two factors (ANOVA 18:4n-3: $F_{1,46}$=23.22, P=1.61×10^{-5}; EPA: $F_{1,46}$=13.00, P=7.64×10^{-4}). These ratios were higher in LH groups than in HH fish, and were significantly highest in the LH12 group.

The DHA ratio was significantly affected only by diet, and reached a ratio value of about 8 in LH groups, which was about 4 times higher than for the HH groups (ANOVA temperature: $F_{1,46}$=2.90, P=0.09; food: $F_{1,46}$=25.12, P=8.46×10^{-6}, food×diet: $F_{1,46}$=0.27, P=0.60).

Growth and body condition

The TGC was significantly affected by temperature (ANOVA: $F_{1,104}$=140.62, P=~2×10^{-16}; Table 2), and was higher at 20°C than at 12°C; however, it was not affected by diet (ANOVA: $F_{1,104}$=0.03, P=0.85) or by an interaction between temperature and food (ANOVA: $F_{1,104}$=1.19, P=0.28). The fish growth curves according to time are presented in Fig. S2.

The three body condition indices (FI, HSI and CSI) were significantly affected by temperature. The condition index FI was significantly higher for fish reared at 20°C (ANOVA: $F_{1,53}$=24.31, P=8.48×10^{-6} ; Table 2), while HSI and CSI were significantly higher for the 12°C groups (ANOVA HSI: $F_{1,50}$=5.93, P=1.85×10^{-2}; CSI: $F_{1,50}$=4.70, P=0.03; Table 2). None of these parameters were affected by food (ANOVA HSI: $F_{1,50}$=2.68, P=0.11; FI: $F_{1,53}$=0.24, P=0.62; CSI: $F_{1,50}$=0.08, P=0.77) or by an interaction between food and temperature (ANOVA HSI: $F_{1,50}$=3.11, P=0.08; FI: $F_{1,53}$=1.08, P=0.30; CSI: $F_{1,50}$=2.90, P=0.09).

Swimming performance, energetics and blood parameters

As expected, $\dot{M}_{O_2}$ increased exponentially with swimming speed (data not shown). The effects of diet and temperature on U_{crit}, SMR, MMR, AS, NCOT and haematocrit are summarised in Table 2.

U_{crit} was not affected by diet (ANOVA: $F_{1,49}$=0.05, P=0.83), temperature (ANOVA: $F_{1,49}$=2.34, P=0.13) or an interaction between the two (ANOVA: $F_{1,49}$=1.34, P=0.25).

SMR and NCOT were both affected by temperature: the 20°C groups showed an approximately 33% lower SMR (ANOVA: $F_{1,48}$=11.92, P=0.1×10^{-2}) and a NCOT almost twice as high as that of the 12°C groups (ANOVA: $F_{1,44}$=65.50, P=2.97×10^{-10}). SMR and NCOT were not affected by food (ANOVA SMR: $F_{1,48}$=0.28, P=0.60; NCOT: $F_{1,44}$=0.09, P=0.76) or by an interaction between food and temperature (ANOVA SMR: $F_{1,48}$=3.99, P=0.05; NCOT: $F_{1,44}$=0.81, P=0.37).

Journal of Experimental Biology (2019) 222, jeb187179. doi:10.1242/jeb.187179

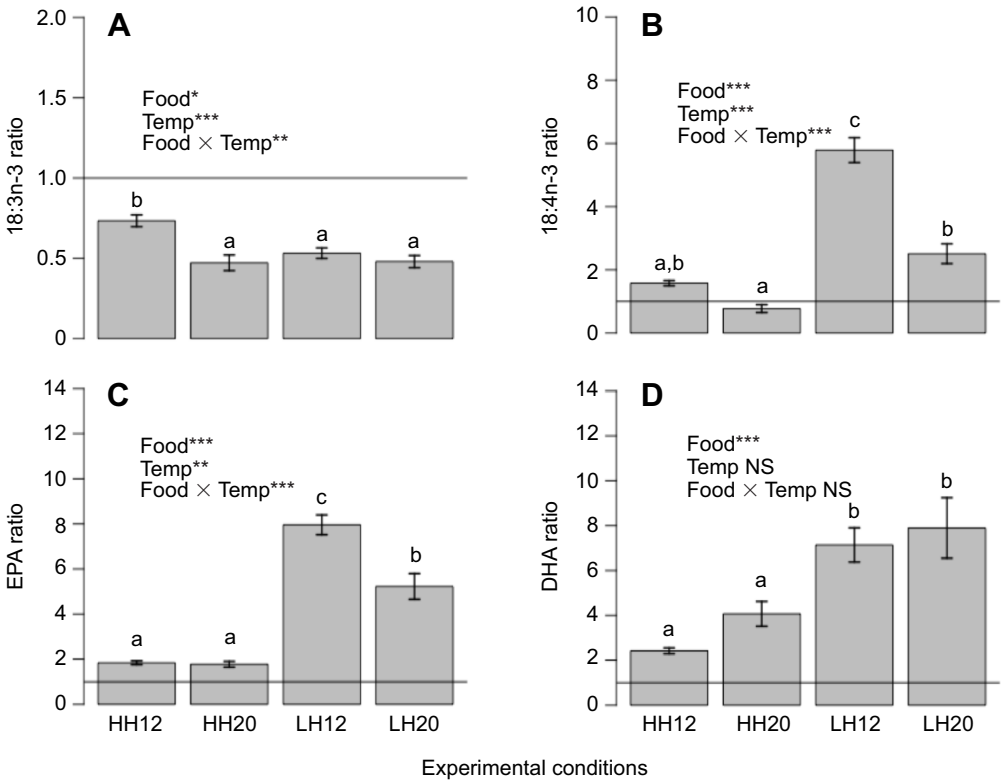

Fig. 1. Fatty acid (FA) ratio between fish muscle and food in *Chelon auratus*. Change in fish FA muscle content to dietary FA content ratio for linolenic acid (18:3n-3), stearidonic acid (18:4n-3), eicosapentaenoic acid (EPA; 20:5n-3) and docosahexaenoic acid (DHA; 22:6n-3) for each experimental group (HH12, LH12, HH20, LH20; n=13 per experimental condition) tested and reared at 12 or 20°C and fed the high HUFA (highly unsaturated fatty acids of the omega-3 series) diet (HH) or the low HUFA diet (LH). The horizontal lines indicate the 1:1 ratio. Statistical significance of food, temperature and the interaction between the two factors is indicated in each panel: *P<0.05, **P<0.01, ***P<0.001; NS, non-statistical significance of the factor (two-way ANOVA). For further statistical details, see Results.

Both MMR and AS were affected by temperature (ANOVA MMR: $F_{1,45}$=47.88, P=1.34×10^{-08}; AS: $F_{1,43}$=68.76, P=1.84×10^{-10}), and were globally higher at 20°C than at 12°C. They were also affected by an interaction between temperature and diet, and were significantly highest in the LH20 group and lowest in the LH12 group (ANOVA MMR: $F_{1,45}$=6.31, P=0.02; AS: $F_{1,43}$=5.90, P=0.02). Neither MMR nor AS was affected by food (ANOVA MMR: $F_{1,45}$=0.03, P=0.90; AS: $F_{1,43}$=0.02, P=0.90).

Haematocrit was 20% higher in the 20°C groups than in the 12°C groups (ANOVA: $F_{1,45}$=9.01, P=0.4×10^{-2}), and 13% higher in HH than in LH groups (ANOVA: $F_{1,45}$=5.96, P=0.02), but there was no interaction between temperature and food (ANOVA: $F_{1,45}$=0.54, P=0.46).

Cardiac performance

Under control conditions (10 nmol l^{-1} adrenaline; Fig. 2D), the pumping capacity increased to its maximum value before slightly decreasing at high frequencies, whatever the group (Lmer: frequency effect: χ^2_1=101.8, P=2.2×10^{-16}). The 12°C groups exhibited a significantly higher pumping capacity (Lmer: χ^2_1=7.5, P=0.6×10^{-2}; Fig. 2D), which reached a maximal value at lower stimulation frequencies than for the 20°C groups (1.08 ±0.40 Hz for 12°C groups versus 1.43±0.18 Hz for 20°C groups; median±IQR; Fig. 3; ANOVA: F_1=14.7, P=0.3×10^{-3}). Neither an effect of diet (Lmer: χ^2_1=1.2; P=0.28) nor any interactions between the factors tested was observed on pumping capacity (P>0.05).

Conversely, peak tension and half-relaxation rates were particularly affected by an interaction between temperature, diet and frequency, and were highest in LH12 fish (Fig. 2B,C). Both of these variables tended to be lowest at high frequencies (peak tension, interaction temperature×frequency×food: χ^2_1=6.83, P=0.9×10^{-2}; half-relaxation rate, temperature×frequency×food: χ^2_1=7.1, P=0.8×10^{-2}).

The contraction rate was affected by an interaction between food and frequency (lmer: food×frequency: χ^2_1=21.3, P=3.9×10^{-6}), as well as by an interaction between temperature and frequency (temperature×frequency: χ^2_1=12.5, P=0.4×10^{-3}; Fig. 2A). It tended to be highest in the 12°C groups, especially at 0.5 and 1 Hz, and highest in the LH groups, especially under 1 Hz, for each temperature considered.

After the addition of a high adrenaline concentration (10 µmol l^{-1}; Fig. 4), the four variables varied greatly depending on the pacing frequency (lmer: half-relaxation rate χ^2_1=5.9, P=0.02; peak tension χ^2_1=36.2, P=1.7×10^{-9}; pumping capacity χ^2_1=32.7, P=1.1×10^{-8}; contraction rate χ^2_1=24.6, P=7.2×10^{-7}). The variation in contraction rate was significantly affected by the interaction between pacing frequency and food (lmer χ^2_1=5.9; P=0.02). No effect of temperature was observed on these variables (P>0.05).

The blocking of ryanodine receptors by adding ryanodine induced a decrease in peak tension in all groups compared with control conditions (i.e. after basal 10 nmol adrenaline level injection; Fig. 5A), whatever the pacing frequency (all curves below the 0% variation line); however, this decrease was more marked in the 12°C groups than in the 20°C groups, and particularly below 1 Hz (lmer: temperature×frequency: χ^2_1=14.06; P=1.77×10^{-4}).

Following 10 µmol l^{-1} adrenaline injection (Fig. 5B), the addition of ryanodine significantly reduced the peak tension in all groups, except for the LH20 group, which demonstrated a relatively stable peak tension when stimulated from 1 to 2 Hz (points near the 0% variation; lmer: temperature×food: χ^2_1=3.95, P=0.04; temperature×frequency: χ^2_1=15.96, P=6.46×10^{-5}).

Transcriptomic response: RNAseq

Quality of the transcriptome assembly

De novo transcriptome assembly yielded 328,877 transcripts with a contig N50 of 1474 bp. Most (92.1%) quality-filtered reads mapped

Journal of Experimental Biology (2019) 222, jeb187179. doi:10.1242/jeb.187179

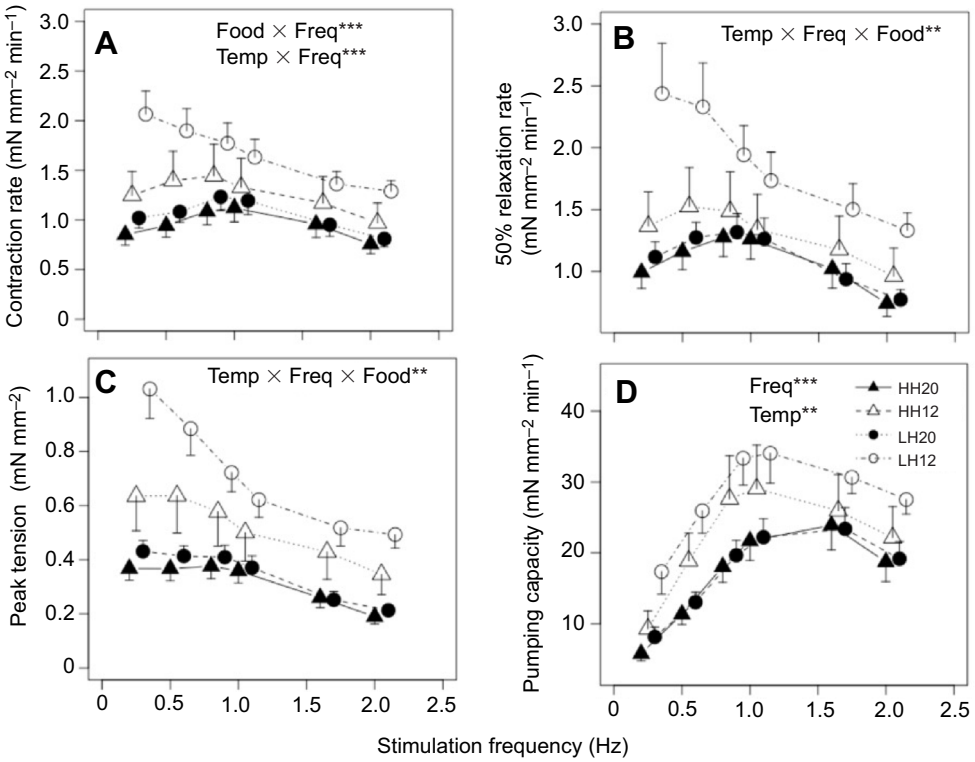

Fig. 2. Cardiac performance. Contraction rate (A), 50% relaxation rate (B), peak tension (C) and pumping capacity (D) of *C. auratus* isolated ventricular strips following treatment with low (10 nmol) adrenaline. Strips were tested at the respective acclimation temperature of fish (12 or 20°C). Data (means±s.e.m.) are presented according to the pacing frequency (Hz) applied to the heart tissue for each experimental group (HH20 n=15, LH20 n=17, HH12 n=20, LH12 n=7) tested and reared at 12 or 20°C and fed the HH or the LH diet. The statistical significance (α=0.05) of temperature, pacing frequency and food, as well as their potential interactions (linear mixed effect model with individual as random factor) is indicated in each panel: **P<0.01, ***P<0.001.

back to the assembly. Transcriptome assembly was successful as most genes conserved among eukaryotes (95.7%), metazoans (95%) and actinopterygians (74.4%) were recovered in our assembly (BUSCO v3; Simão et al., 2015; Waterhouse et al., 2018).

Differential expression levels

Transcription levels differed mostly between temperature treatments (Fig. 6). At high HUFA levels [false discovery rate (FDR) threshold of 5%], 3.77% (n=2319) and 1.4% (n=860) of transcripts were respectively up- and down-regulated at 20°C versus 12°C. A similar pattern was observed at low HUFA levels (4.68% and 1.88% transcripts up- and down-regulated, respectively). Expression changes between temperature treatments (measured as $\log_2$ fold-change, logFC) varied between −10 and 8.9 (median: −3.7) at high HUFA levels, and between −9.1 and 10.1 (median: −2.6) at low HUFA levels. No differentially expressed transcripts were detected between HUFA treatments, regardless of the temperature.

However, we observed an interaction between temperature and diet, as 4.63% and 1.85% of transcripts were up- and down-regulated at LH20, compared with HH12. Similarly, 3.42% and 1.34% of transcripts were up- and down-regulated at HH20, compared with LH12. In these cases, expression changes were of the order of −9.4 and 9.5 logFC (median: −1.1). When considering all differentially expressed genes found between temperature treatments, we observed that the median logFC was significantly stronger for up-regulated genes (−4) than for down-regulated ones (1.5; Wilcoxon rank sum test on absolute values: P<0.001). In summary, an increase in temperature resulted in more up-regulated transcripts with stronger fold-change than down-regulated transcripts. A large proportion of the transcripts mobilised in this response to increased temperature were the same, whether diet varied or not, and ranged between 27.5% of transcripts in common between the HH20–LH12 and HH12–LH20 comparisons and 51.1% of transcripts in common between the HH12–LH20 and HH12–HH20 comparisons (Fig. 7; for logFC>2).

Among all comparisons between different temperatures (HH12–HH20, LH12–LH20 and HH12–LH20; ignoring the LH12–HH20 comparison as it is ecologically improbable), identified genes up-regulated at 20°C are involved in muscle contraction (e.g. Myosin-7 and -10 isoforms; logFC between 2.44 and 7.32). At this temperature, we also detected up-regulation of a Ras-related gene (RAB44; logFC between 6.55 and 10.02), coding for a protein belonging to the plasma membrane, involved in intra-cellular membrane transport and enabling calcium ion binding.

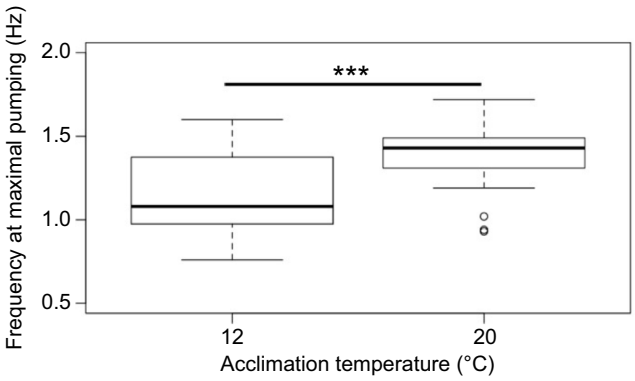

Fig. 3. Effect of acclimation temperature on maximum pumping. Boxplot showing the stimulation frequency at which the maximum pumping capacity was obtained in isolated ventricular strips tested at their respective acclimation temperature (12 or 20°C) from *C. auratus* previously acclimated at 12°C (n=27) or 20°C (n=32). The statistical significance (α=0.05) of acclimation temperature is indicated: ***P<0.001.

Enriched GO terms

At low HUFA, a total of 486 GO terms were significantly enriched (FDR threshold of 5%; Tables S2, S3) among differentially

Journal of Experimental Biology (2019) 222, jeb187179. doi:10.1242/jeb.187179

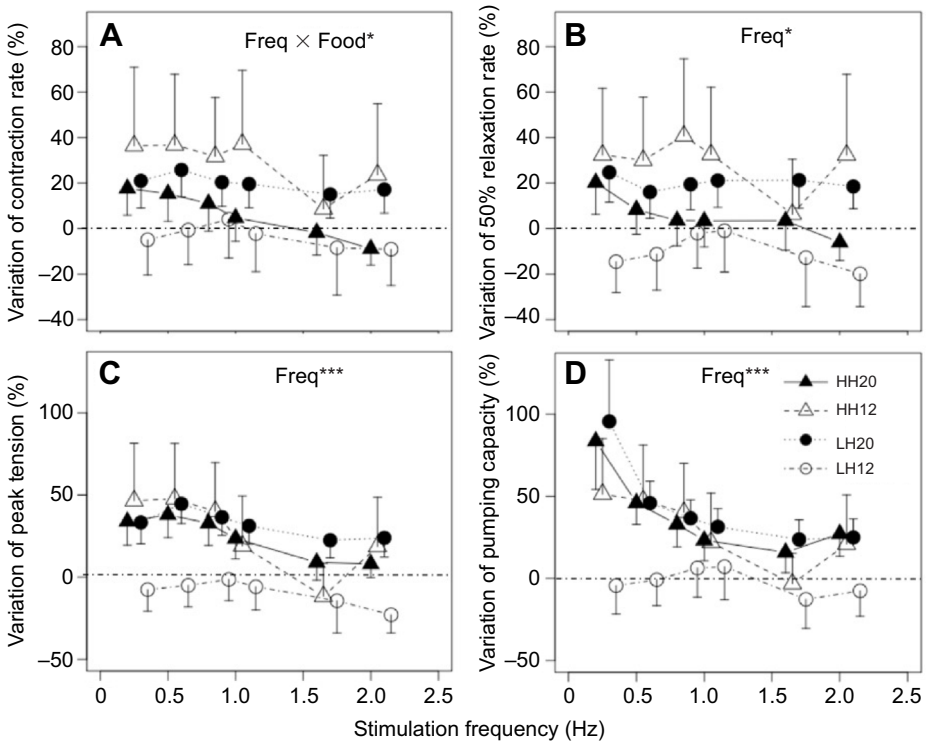

Fig. 4. Effect of adrenaline on cardiac performance. Variation of contraction rate (A), 50% relaxation rate (B), peak tension (C) and pumping capacity (D) of *Chelon auratus* isolated ventricular strips following treatment with high adrenaline solution (10 µmol) compared with the basal circulating adrenaline level (10 nmol). Strips were tested at the respective acclimation temperature of fish (12 or 20°C). For each of the four cardiac variables measured, the horizontal line indicates 0% variation between the values obtained under 10 µmol adrenaline treatment (high adrenaline solution) and those obtained under 10 nmol adrenaline treatment (basal adrenaline solution). Higher values obtained under 10 µmol adrenaline solution compared with those under the basal adrenaline level, suggesting high adrenergic sensitivity, are indicated above this line, while lower values obtained under 10 µmol adrenaline solution compared with the basal adrenaline level, suggesting low adrenergic sensitivity, are indicated below this line. Data (means±s.e.m.) are presented for each pacing frequency (Hz) tested on the heart tissue for each experimental group (HH20 n=15, LH20 n=17, HH12 n=20, LH12 n=7) tested and reared at 12 or 20°C and fed the high HUFA diet (HH) or the low HUFA diet (LH). The statistical significance (α=0.05) of temperature, pacing frequency and food, as well as their potential interactions (linear mixed effect model with individual as random factor) are indicated in each panel: *P<0.05, ***P<0.001.

expressed transcripts between the 12 and 20°C temperature treatments (LH12–LH20 comparison). At high HUFA, 99 GO terms were enriched among differentially expressed transcripts between 12 and 20°C (HH12–HH20 comparison).

There were 73 common GO terms between the HH12–HH20 and LH12–LH20 comparisons (Fig. 7). These 73 GO terms represented 74% (i.e. 73/99 GO terms) of the total GO terms for HH12–HH20, but only 15% (i.e. 73/486 GO terms) of the total GO terms for LH12–LH20. In other words, 85% (413/486) of the enriched GO terms detected for the LH12–LH20 comparison were only detected in that specific comparison, while only 36% (26/99) of the enriched GO terms detected for the HH12–HH20 comparison were only detected in that specific comparison. Therefore, the functional response to temperature elevation was more specific at low HUFA than at high HUFA (Fig. 7A). Similarly, there were more significantly enriched GO terms associated with the HH12–LH20 comparison (n=311) than with the HH12–HH20 comparisons (99 GOs). The functional response for HH12–LH20 was more specific (24% of enriched GO terms in common with HH12–HH20) than that for HH12–HH20 (77% of enriched GO terms in common with HH12–LH20; Fig. 7). Depleted GO terms were never detected among these comparisons.

Four classes of biological processes recurred in all comparisons: cytoskeleton organisation, transmembrane transport (including ion transport and metal ion transport), actin filament processes and regulation of heart and muscle contraction. In all comparisons, cellular components included contractile fibre part, sarcolemma and cell junctions. Finally, molecular functions mainly included motor activity, actin or protein binding, potassium channel regulatory activity and ion transmembrane transport activity. The 73 enriched GO terms found in common between the HH12–HH20 and LH12–LH20 comparisons were reduced to key biological processes summarised as the regulation of heart rate (including action potential, positive regulation of ion transmembrane transport including calcium, ATPase activity and muscle contraction), cytoskeletal organisation and membrane assembly, and actin filament-based processes (including striated muscle cell development and cytokinesis). Cellular components included the contractile fibre part, myosin filaments, the cytoskeleton and sarcolemma, as well as cell contact zones. Molecular functions mainly involved protein binding (calmodulin, actin, ankyrin and cytoskeletal protein binding), motor activity and sodium transmembrane transporter activity.

We then looked at the 235 enriched GOs that were specific to the HH12–LH20 comparison, when compared with HH12–HH20; these GO terms are linked to the combined effect of elevated temperature and lowered concentration of HUFA in the diet (Fig. 8, Table 1). These GO terms pertained mainly to processes involving muscle contraction and development, cytoskeletal dynamics and transmembrane dynamics (Fig. 8, Table 1). More specifically,

Journal of Experimental Biology (2019) 222, jeb187179. doi:10.1242/jeb.187179

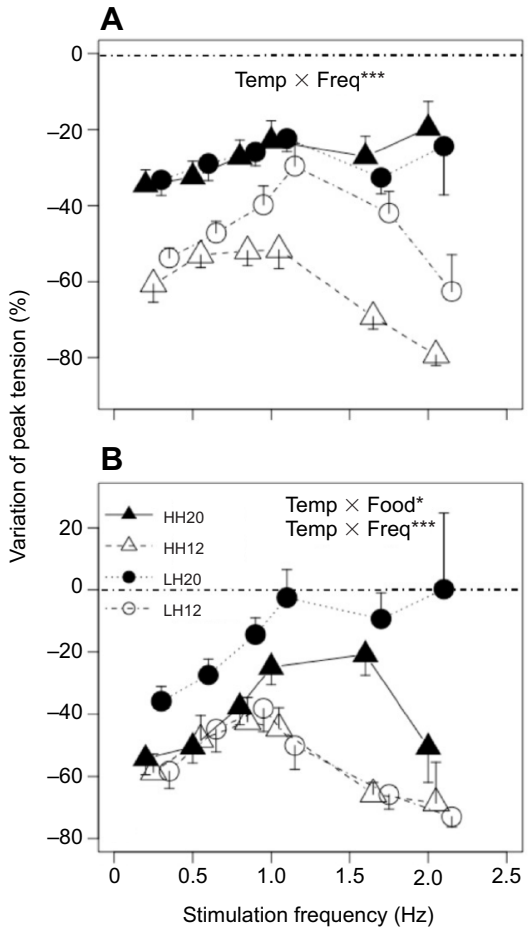

Fig. 5. Effect of ryanodine. Variation in peak tension obtained under treatment with ryanodine solution added to a basal adrenaline level (10 nmol) compared with the basal circulating adrenaline level (10 nmol) (A) or added to adrenaline solution (10 µmol) compared with the stimulating adrenaline level (10 µmol) (B). Ventricular strips were tested at their respective acclimation temperature (12 or 20°C). For each panel, the horizontal line indicates 0% variation between the values obtained under ryanodine added to adrenaline (adrenaline) treatment and those obtained under adrenaline treatment alone. Adding ryanodine blocks the ryanodine receptors present on the sarcoplasmic reticulum (SR), resulting in a decrease in peak tension compared with control conditions. Thus, the more negative the value, the more the peak tension decreased as a result of the lack of SR contribution, revealing the usually high SR contribution. Data (means±s.e.m.) are presented according to the stimulation frequency (Hz) applied to the heart tissue for each experimental group ([HH20 n=15, LH20 n=17, HH12 n=20, LH12 n=7) tested and reared at 12 or 20°C and fed the HH or the LH diet. The statistical significance (α=0.05) of temperature, stimulation frequency and food, as well as their potential interactions (linear mixed effect model) are indicated in each panel: *P<0.05, ***P<0.001.

among the 165 enriched GO terms pertaining to biological processes (including heart muscle contraction, the regulation of ion transmembrane transport and cytoskeleton organisation), 14 involved calcium-mediated processes, such as the regulation of voltage-gated calcium channel activity (GO:1901385, including 11 differentially expressed transcripts), the positive regulation of calcium-transporting ATPase activity (GO:1901896, including seven differentially expressed transcripts), calcium ion transmembrane transport via high voltage-gated calcium channel (GO:0061577, including four differentially expressed transcripts), regulation of cardiac muscle contraction by regulation of the release of sequestered calcium ion (GO:0010881, including 16 differentially expressed transcripts) and regulation of the release of sequestered calcium ion into cytosol through sarcoplasmic reticulum (GO:0010880, including 21 differentially expressed transcripts). Among the 33 differentially expressed transcripts involved in these processes (26 transcripts are involved in more than one GO term), isoforms of the Ryanodine receptor 2 (RYR2; logFC ranging between 2.95 and 7.71) and the voltage-dependent L-type calcium channel subunit alpha 1C (CAC1C; logFC 4.11-6.64) were the most strongly up-regulated at 20°C. We also detected isoforms of Ankyrin (ANK2 and ANK3; logFC 2.58-5.71), which modulates the attachment of actin to the cytoskeleton (differentially expressed transcripts are presented in Table S4). REVIGO also detected many GO terms associated with morphogenesis (anatomical structure, neuron projection, hypochord, cardiac muscle tissue morphogenesis, adult heart development). Similarly, for cellular components, GO terms were associated with the cell membrane (T-tubules, polysynaptic membrane, plasma membrane region, cell–cell junctions, cell surface furrow, calcium and sodium channel complexes). A large proportion of GO terms involved in molecular function were linked to binding (e.g. cadherin binding, S100 protein binding, ion channel binding, cell adhesion molecule binding), structural molecule activity conferring elasticity and the structural constituent of the cytoskeleton.

DISCUSSION

Using an integrative approach, this study offers insights into the underlying mechanisms governing the fish cardio-respiratory phenotype in response to temperature and lowering HUFA food content. It reveals that the metabolic effects observed at the individual level may result from the modification of heart tissue functioning, particularly at high levels of effort.

The selective retention of EPA and DHA in LH fish shows that the HUFA content supplied by the LH diet was not enough to cover the requirements in fish tissue, confirming the HUFA deficiency in the LH diet. Conversely, the HH diet supplied enough HUFA to cover the requirements of fish tissue, as shown by the HUFA ratio between muscle and diet, which was always near one or above.

Heart tissue performance depends on the temperature and effort considered

Temperature explained most of the variation in individual, physiological, systemic and molecular responses observed in fish acclimated at 12 and 20°C (e.g. Fig. 6). Thus, and not surprisingly, the 20°C acclimation temperature increases the metabolism (MMR and AS) and energy allocation to physiological performance, such as growth (TGC and FI index) (Claireaux and Lagardère, 1999; Fry, 1971).

Interestingly, fish acclimated at 12°C showed (i) a higher SMR than those acclimated at 20°C and, concomitantly, (ii) improved cardiac performance under the basal adrenaline level. This was shown by a higher pumping capacity, peak tension, relaxation rate and ability to reach a maximum pumping capacity at lower frequency than the 20°C groups. This effect of temperature on cardiac performance is in accordance with what has already been reported in rainbow trout (Keen et al., 1994). Similarly, as is usually found (Driedzic and Gesser, 1994; Gamperl, 2004; Keen et al., 2017), the better performance at a colder temperature was associated with a larger heart (CSI) in the present study. This would compensate for the higher blood density at low temperature by increasing the pumping capacity in order to supply blood through the entire organism (Keen et al., 2017). This increase in heart mass at low temperature is usually attributed to hyperplasia

Journal of Experimental Biology (2019) 222, jeb187179. doi:10.1242/jeb.187179

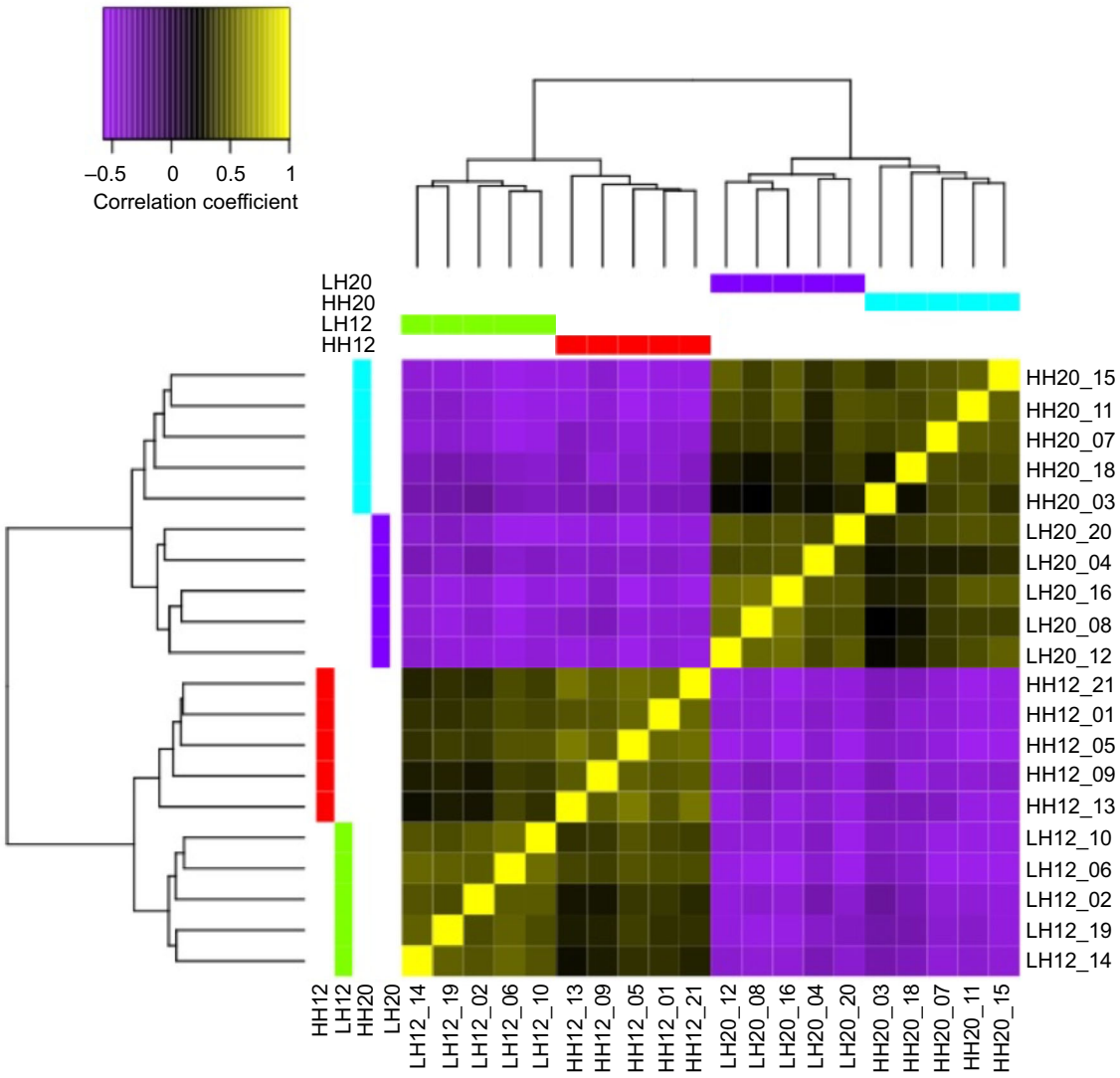

Fig. 6. Differential expression of transcripts between groups. Correlogram displaying Pearson's correlation coefficients based on expressed transcripts between pairs of sample replicates within and across the four treatments (LH12, HH12, LH20 and HH20; *n*=5 samples per experimental condition). The clustering of sample replicates (left row and top column dendrograms) was constructed using the Pearson correlation matrix. The associated colour bars (displayed at the tips of each dendrogram) represent experimental treatments (the key is indicated next to the colour bars). Sample replicates are indicated on rows (right) and columns (bottom). The colour key of the heatmap (top left of the figure) indicates the value of the Pearson's correlation coefficient.

(increased cell numbers) and/or hypertrophy (increased myocyte size) resulting from a more efficient protein and/or FA synthesis or degradation (Driedzic and Gesser, 1994; Gamperl, 2004; Keen et al., 2017). Accordingly, in our study, biological processes involved in muscle cell development (GO:0055001) and striated muscle development (GO:0055002) were significantly enriched in all comparisons involving temperature (HH12 versus HH20, HH12 versus LH20, LH12 versus HH20, LH12 versus LH20; Table S3).

This cardiac remodelling at low temperature was also associated with a decreasing peak tension in the presence of ryanodine. From a functional standpoint, this indicates that the cardiac contraction at 12°C depends more on the mobilisation efficiency of intracellular Ca^{2+} stored in the SR than on an extracellular Ca^{2+} source. This increase in the SR channel contribution to Ca^{2+} mobilisation, as usually found in cold-acclimated fish (Imbert-Auvray et al., 2013; Keen et al., 1994; Shiels et al., 2002; Vornanen, 1996, 1998) could be explained by a SR proliferation in heart cells (Bowler and Tirri, 1990; Keen et al., 1994, 2017; Shiels and Farrell, 1997; Shiels et al., 2011), a higher ryanodine sensitivity (Vornanen et al., 2005) and/or a partial (or complete) inactivation, due to cold, of the SL channels/exchanger allowing extracellular Ca^{2+} influx into the cells (Vornanen, 1998; Vornanen et al., 2002).

Cardiac remodelling at low temperature is thus demonstrated in *C. auratus*, but this remodelling may have a cost, as suggested by the higher SMR measured at 12°C versus 20°C. However, the causative relationship between cardiac remodelling and elevated SMR remains to be fully investigated.

Moreover, higher cardiac performance and oxygen consumption were observed in LH12 fish versus HH12 fish under physiological conditions (low adrenaline level). This indicates that the assumptions made above to explain a higher cardiac performance in cold-acclimated fish compared with 20°C-acclimated fish cannot be the only processes involved, and that diet interacts with temperature to affect performance. The higher cardiac performance of LH12 versus HH12 could be the result of the use of saturated and monounsaturated FA as major metabolic fuels,

Journal of Experimental Biology (2019) 222, jeb187179. doi:10.1242/jeb.187179

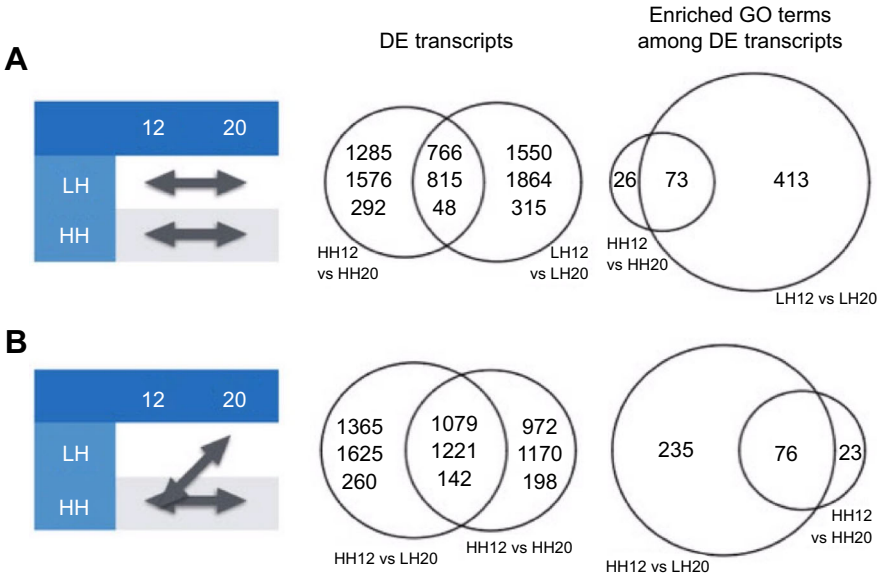

Fig. 7. Venn diagrams showing the number of differentially expressed transcripts and enriched gene ontology (GO) terms detected for different treatment comparisons. *n*=5 samples per experimental condition. The tables on the left represent the treatment comparisons based on which differential expression and GO enrichment analysis were conducted. Treatment comparison is symbolised by arrows in the tables: (A) LH12–LH20, HH12–HH20; (B) HH12–LH20, LH12–HH20. Each circle in the Venn diagrams represents the number of differentially expressed (DE) transcripts (left) or enriched GO terms (right) detected within a treatment comparison (i.e. arrows in the tables). The Venn diagram informs us of the proportion of differentially expressed transcripts or enriched GO terms that are specific to a treatment comparison, or shared between two comparisons (intersection between two circles). In the Venn diagrams corresponding to the differentially expressed transcripts, the number of up-regulated (top number) and down-regulated (bottom number) transcripts, and the total number of differentially expressed transcripts (centre number) are given for each comparison. Comparisons between HUFA treatments at low and high temperatures (LH12 versus HH12 and LH20 versus HH20) are not presented as no differentially expressed transcripts were detected among these groups. The LH12 versus HH20 comparison is not shown as this scenario was considered ecologically improbable.

preferred over HUFA, and highly present in the LH diet (Chatelier et al., 2006; Egginton, 1996; Henderson and Sargent, 1985; McKenzie, 2001). Conversely, there is no indication of the preferential use of different metabolic fuels in LH20 versus HH20 groups, as fish exposed to these two 20°C conditions demonstrated similar heart performance.

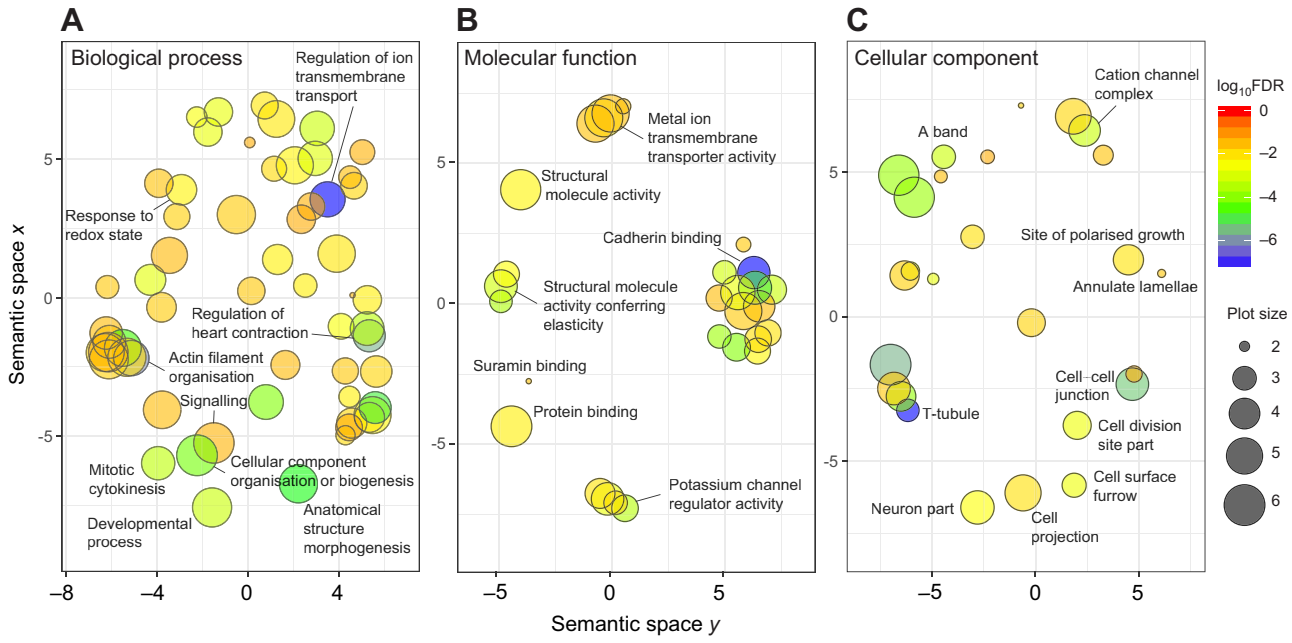

Fig. 8. REVIGO summary based on the GO term enrichment analysis performed for the treatment comparison HH12 and LH20. *n*=5 samples per experimental condition. The three bubble diagrams correspond to biological processes (A), molecular functions (B) and cellular components (C). Bubbles represent the GO terms remaining after the REVIGO redundancy reduction, plotted in two-dimensional space, based on the semantic similarity among GO terms. Bubble colour indicates the significance of the enrichment tests (scale of $\log_{10}$ of the false discovery rate, $\log_{10}$FDR, presented on the right). Bubble size indicates the frequency of representative GO terms in the underlying UniProt GO annotation database (the bigger the bubble, the more general the GO term; the smaller the bubble, the more specific).

Temperature and HUFA availability in food exert an interactive effect on heart tissue performance

This study clearly demonstrates that the significant changes observed among the physiological, cardiac and molecular variables measured between 12 and 20°C were exacerbated by a lower HUFA availability (LH12–LH20 treatments). In particular, the mechanisms involved in Ca^{2+} mobilisation capacity during excitation–contraction coupling appear specific to the LH20 group compared with the other groups, and especially compared with the LH12 group.

In more detail, LH20 fish demonstrated a reduction of peak tension due to blocked ryanodine receptors, which was compensated for by the application of a high adrenaline dose (10 µmol l^{-1}) from 1 Hz. Firstly, this could reflect the increased adrenergic sensitivity of the ventricular tissue through an increase of β-adrenergic receptor density (Gamperl, 2004; Keen et al., 1994). Secondly, this suggests that the LH20 ventricle can increase its force-generating ability by increasing extracellular Ca^{2+} influx via sarcolemmal channels. A differential expression of genes involved in Ca^{2+} membrane transport via high voltage-gated calcium channels (such as L-type channels) supported this specific cardiac muscle contractility process in LH20 [GO:0061577 detected among the 235 enriched GO terms that were specific to the HH12–LH20 comparison (Fig. 7B, 8) and therefore indicative of the combined effect of high temperature and low HUFA dietary content]. Complementarily, a higher number of transcripts encoding L-type and ryanodine receptors were found in that group compared with the others (Table S4). Moreover, GO terms involving the SR were only significantly enriched (i.e. process over-represented among differentially expressed transcripts) in comparisons involving LH20 (LH12–LH20 and HH12–LH20 comparisons). In particular, the biological process named regulation of release of sequestered Ca^{2+} into cytosol by sarcoplasmic reticulum (GO:0010880) was detected for both comparisons (Table S2, S3). Thus, combining data from physiological tests (exposure to ryanodine and adrenaline under cardiac stimulation) and transcriptomics (expression levels of Ca^{2+} channels) suggests that, under stressful conditions (10 µmol l^{-1} adrenaline), the low HUFA diet promotes heart contraction in warm-acclimated fish through a Ca^{2+} mobilisation depending probably on both the adrenergic pathway via SL channels and SR Ca^{2+} stores.

This strategy of LH20 fish was associated with the highest MMR and AS in our study, but also a relatively higher NCOT to swim at U_{crit}. From a metabolic standpoint, this suggests that fish reared in LH20 conditions utilise a more expensive cardiac strategy. In their natural environment, fish face several energy-demanding activities concomitantly to swimming, such as digestion, growth or escape from predators (Fry, 1971). All these activities are mainly governed by the heart's capacity to supply oxygen to tissues (Claireaux, 2005; Clark et al., 2005). Even though our results were obtained experimentally, without any constraints on foraging or predator risk related to the natural environment, they suggest that cardiac strategies for Ca^{2+} mobilisation set up by LH20 fish may not be optimal and may have ecological consequences, such as a reduction in further long-term growth.

Conversely, the LH12 hearts showed the highest peak tension and half-relaxation rate, especially at low pacing frequencies, under basal metabolic conditions (Fig. 2). This suggests a more efficient Ca^{2+} mobilisation during excitation–contraction coupling in these hearts. Concomitantly, the decreasing peak tension under ryanodine treatment added to the basal adrenaline dose (10 nmol l^{-1}) and the enrichment of GO:0010880 (regulation of release of sequestered Ca^{2+} ion into cytosol by sarcoplasmic reticulum) in differentially expressed transcripts in the LH12–LH20 and HH12–LH20 comparisons support a high SR involvement in Ca^{2+} mobilisation in LH12 hearts (Tables S2 and S3).

Interestingly, at all pacing frequencies, LH12 cardiac performance was not significantly modulated under stressful conditions (10 µmol l^{-1} adrenaline) compared with that observed under 10 nmol l^{-1} adrenaline (i.e. no significant variation in the contraction rate, peak tension relaxation rate and pumping capacity; Fig. 4). This suggests a limited capacity to mobilise extracellular Ca^{2+} to maintain ventricle contraction, and thus a low adrenergic sensitivity in this group. The SR contribution also seems to be reinforced under stressful conditions in LH12, as shown by the more intense reduction of peak tension by ryanodine in 10 µmol l^{-1} adrenaline pre-treated ventricles. Even if not significant, this SR contribution would tend to compensate for the low adrenergic sensitivity of the LH12 group at all pacing frequencies, shown by stable cardiac performance under adrenaline stimulation (10 µmol l^{-1}).

Taken together, these results suggest that lowering HUFA availability combined with high temperature induces (1) a proliferation of SL and SR Ca^{2+} channels and (2) a higher force-generating ability by increasing extracellular Ca^{2+} influx via sarcolemmal channels when the heart has to sustain excessive effort due to stress and/or exercise. The same diet given at low temperature, however, would induce a lower adrenergic sensitivity with a higher SR contribution, increasing under stressful conditions. In addition, while no enriched GO term corresponding to transmembrane receptors was detected, 11 biological process GO terms pertaining to the regulation of ion transmembrane transport (GO:0034765) were enriched in LH20 versus HH12 and LH12. Similarly, the plasma membrane cellular component (GO:0005886) was significantly involved. Finally, multiple GO terms involved in ion channel regulation (GO:0015459, GO:0016247, GO:0022838, GO:0022836, GO:0008514) were significantly enriched in the comparisons involving LH20 (LH12–LH20 and HH12–LH20; Table S2; Fig. 8).

One hypothesis to explain such results could be that the lesser dietary supply in EPA and DHA in LH groups versus HH groups, reflected in muscle tissue (Vagner et al., 2015), could also have impacted the membrane composition of cardiomyocytes (in which the sarcolemmal channels are embedded) and that of sub-cellular organelle membranes, such as the SR (in which the ryanodine receptors are embedded) (Porter et al., 1996). This lesser HUFA content may have then impacted the functionality of the embedded channels and receptors, as shown in other species (Turner et al., 2003; Ushio et al., 1997). The transcriptomic results support this hypothesis, showing the significant enrichment of GO:0044325, involved in ion channel regulation, in the comparisons involving the LH diet (i.e. HH12–LH20, LH12–LH20, LH12–HH20; Table S3).

The differences in cardiac performance observed between LH20 and LH12 fish could result from the different contribution to the Ca^{2+} pool of the two membrane sub-types (sarcolemmal and organellar), the HUFA composition of which varies with both acclimation temperature and energetic demand (Bell et al., 1986). While the DHA content was similarly low in the two LH groups, lipid analysis previously performed on fish muscle demonstrated that the LH diet induced a lower EPA content in muscle membranes at 20°C than at 12°C (Vagner et al., 2015). This lower EPA content in LH20 fish could be a response to increasing temperature with a decreasing degree of unsaturation known to preserve the membrane fluidity (Person-Le Ruyet et al., 2004; Raynard and Cossins, 1991; Wodtke, 1991).

According to the abundant literature reporting that dietary FA shapes heart FA composition in fish (Bell et al., 1991, 1993; Lopez-Jimena et al., 2015; Thomassen and Røsjø, 1989), we assume that the cardiomyocyte cell and sub-cellular membranes of LH20 fish also demonstrated a low EPA content, as found in their muscle. The different receptor/channel transcription and functionality demonstrated between LH20 and LH12 groups could thus be explained by the lower EPA content in the LH20 groups. Modulation of the calcium pathway by EPA and DHA has been observed in the ventricular myocytes of mammals (O'Neill et al., 2002; Swan, 2003; Turner et al., 2003; Wu et al., 2003; Xiao et al., 1997). For example, in rat ventricular myocytes, an acute treatment with EPA induced inhibition of the cardiac L-type calcium channel (Xiao et al., 1997) and a modulation of SR function in order to participate in this way in the positive antiarrhythmic effects on heart attributed to the SR (O'Neill et al., 2002; Swan, 2003). According to the literature, and to our results, we offer the hypothesis that in *C. auratus*, dietary EPA could be an efficient driver in the functioning of cardiomyocyte membrane sub-types, and that its deficiency in fish cardiomyocytes would result in a higher energetic cost in order to maintain an efficient cardiomyocyte functionality.

This physiological response will probably have detrimental consequences for the fish itself and for the functioning of the whole ecosystem. Our understanding of these processes is still limited, because the lessening HUFA content in food webs remains an understudied factor in the context of global change. Through this original and integrative approach, we hope that this study will spark interest in considering the effects of HUFA availability on ectotherms, given its significant functional interaction with temperature.

Acknowledgements
The authors are very grateful to M. Durollet for her help with fish rearing, and to M. Le Gac and J. Quéré from the DYNECO lab of the Ifremer Institute of Plouzané (France) for lab space and their great help with the preparation of DNA libraries. The authors also thank the two reviewers for their constructive criticism on the manuscript. We thank the bioinformatics platform Toulouse Midi-Pyrenees (Bioinfo GenoToul) for providing help and computing resources.

Competing interests
The authors declare no competing or financial interests.

Author contributions
Conceptualization: M.V., T.L.-L., J.-L.Z.-I.; Methodology: M.V., E.P., T.L.-L., P.Q., E.D., V.H., H.L.D., N.I.A.; Software: M.V., E.P., A.V.; Validation: M.V., E.P., A.V., N.I.-A.; Formal analysis: E.P., N.I.-A.; Investigation: M.V., E.P., A.V.; Data curation: E.P.; Writing - original draft: M.V., E.P., A.V., T.L.-L., J.-L.Z.-I., C.L., N.I.-A.; Writing - review & editing: M.V., E.P., T.L.-L., N.I.-A.; Funding acquisition: E.P., C.L., N.I.-A.

Funding
This work is a contribution to the project ECONAT Axe 1 - Ressources Marines Littorales: qualité et éco-valorisation, funded by the Contrat de Plan Etat-Région and the CNRS and the European Regional Development Fund.

Data availability
Raw sequences from the transcriptomic analysis of cardiac tissue are available from the NCBI Sequence Read Archive (accession numbers SRR8782759–78) and the Transcriptome Shotgun Assembly Sequence Database (accession number GHJK00000000; NCBI BioProject PRJNA528917, BioSample SAMN11249709).

Supplementary information
Supplementary information available online at
http://jeb.biologists.org/lookup/doi/10.1242/jeb.187179.supplemental

References
Arts, M. T., Ackman, R. G. and Holub, B. J. (2001). "Essential fatty acids" in aquatic ecosystems: a crucial link between diet and human health and evolution. *Can. J. Fish. Aquat. Sci.* **58**, 122-137.

Bell, M. V., Henderson, R. J. and Sargent, J. R. (1986). The role of polyunsaturated fatty acids in fish. *Comp. Biochem. Physiol. Part B Comp. Biochem.* **83**, 711-719.

Bell, J. G., McVicar, A. H., Park, M. T. and Sargent, J. R. (1991). High dietary linoleic acid affects the fatty acid compositions of individual phospholipids from tissues of Atlantic salmon (*Salmo salar*): association with stress susceptibility and cardiac lesion. *J. Nutr.* **121**, 1163-1172.

Bell, J. G., Dick, J. R., McVicar, A. H., Sargent, J. R. and Thompson, K. D. (1993). Dietary sunflower, linseed and fish oils affect phospholipid fatty acid composition, development of cardiac lesions, phospholipase activity and eicosanoid production in Atlantic salmon (*Salmo salar*). *Prostaglandins Leukot. Essent. Fatty Acids* **49**, 665-673.

Bolger, A. M., Lohse, M. and Usadel, B. (2014). Trimmomatic: a flexible trimmer for Illumina sequence data. *Bioinformatics* **30**, 2114-2120.

Bowler, K. and Tirri, R. (1990). Temperature dependence of the heart isolated from the cold or warm acclimated perch (*Perca fluviatilis*). *Comp. Biochem. Physiol. A Physiol.* **96**, 177-180.

Brett, J. R. (1964). The respiratory metabolism and swimming performance of young sockeye salmon. *J. Fish. Res. Board Can.* **21**, 1183-1226.

Chatelier, A., Imbert, N., Infante, J. L. Z., McKenzie, D. J. and Bois, P. (2006). Effects of oleic acid on the high threshold barium current in seabass *Dicentrarchus labrax* ventricular myocytes. *J. Exp. Biol.* **209**, 4033-4039.

Claireaux, G. (2005). Linking swimming performance, cardiac pumping ability and cardiac anatomy in rainbow trout. *J. Exp. Biol.* **208**, 1775-1784.

Claireaux, G. and Lagardère, J.-P. (1999). Influence of temperature, oxygen and salinity on the metabolism of the European sea bass. *J. Sea Res.* **42**, 157-168.

Clark, T. D., Ryan, T., Ingram, B. A., Woakes, A. J., Butler, P. J. and Frappell, P. B. (2005). Factorial aerobic scope is independent of temperature and primarily modulated by heart rate in exercising murray cod (*Maccullochella peelii peelii*). *Physiol. Biochem. Zool.* **78**, 347-355.

Clark, T. D., Jeffries, K. M., Hinch, S. G. and Farrell, A. P. (2011). Exceptional aerobic scope and cardiovascular performance of pink salmon (*Oncorhynchus gorbuscha*) may underlie resilience in a warming climate. *J. Exp. Biol.* **214**, 3074-3081.

Crawford, M. A. and Broadhurst, C. L. (2012). The role of docosahexaenoic and the marine food web as determinants of evolution and hominid brain development: the challenge for human sustainability. *Nutr. Health* **21**, 17-39.

Driedzic, W. R. and Gesser, H. (1994). Energy metabolism and contractility in ectothermic vertebrate hearts: hypoxia, acidosis, and low temperature. *Physiol. Rev.* **74**, 221-258.

Egginton, S. (1996). Effect of temperature on optimal substrate for β-oxidation. *J. Fish Biol.* **49**, 753-758.

Fry, F. E. (1971). The effect of environmental factors on the physiology of fish. *Fish Physiol.* **6**, 1-98.

Fulton, T. W. (1904). *The rate of growth of fishes*. In 22nd Annual Report of the Fishery Board of Scotland, pp. 141-241.

Galloway, A. W. E. and Winder, M. (2015). Partitioning the relative importance of phylogeny and environmental conditions on phytoplankton fatty acids. *PLoS ONE* **10**, e0130053.

Gamperl, A. K. (2004). Cardiac plasticity in fishes: environmental influences and intraspecific differences. *J. Exp. Biol.* **207**, 2539-2550.

Gene Ontology Consortium (2004). The Gene Ontology (GO) database and informatics resource. *Nucleic Acids Res.* **32**, D258-D261.

Gladyshev, M. I., Arts, M. T. and Sushchik, N. N. (2009). Preliminary estimates of the export of omega-3 highly unsaturated fatty acids (EPA+DHA) from aquatic to terrestrial ecosystems. In *Lipids in Aquatic Ecosystems* (ed. M. T. Arts, M. T. Brett and M. Kainz)., pp. 179-211. New York: Springer.

Gladyshev, M. I., Sushchik, N. N., Anishchenko, O. V., Makhutova, O. N., Kolmakov, V. I., Kalachova, G. S., Kolmakova, A. A. and Dubovskaya, O. P. (2011). Efficiency of transfer of essential polyunsaturated fatty acids versus organic carbon from producers to consumers in a eutrophic reservoir. *Oecologia* **165**, 521-531.

Glencross, B. D. (2009). Exploring the nutritional demand for essential fatty acids by aquaculture species. *Rev. Aquacult.* **1**, 71-124.

Grabherr, M. G., Haas, B. J., Yassour, M., Levin, J. Z., Thompson, D. A., Amit, I., Adiconis, X., Fan, L., Raychowdhury, R., Zeng, Q. et al. (2011). Full-length transcriptome assembly from RNA-Seq data without a reference genome. *Nat. Biotechnol.* **29**, 644-652.

Haas, B. J., Papanicolaou, A., Yassour, M., Grabherr, M., Blood, P. D., Bowden, J., Couger, M. B., Eccles, D., Li, B., Lieber, M. et al. (2013). De novo transcript sequence reconstruction from RNA-seq using the Trinity platform for reference generation and analysis. *Nat. Protoc.* **8**, 1494-1512.

Henderson, R. J. and Sargent, J. R. (1985). Chain-length specificities of mitochondrial and peroxisomal β-oxidation of fatty acids in livers of rainbow trout (*Salmo gairdneri*). *Comp. Biochem. Physiol. Part B Comp. Biochem.* **82**, 79-85.

Hixson, S. M. and Arts, M. T. (2016). Climate warming is predicted to reduce omega-3, long-chain, polyunsaturated fatty acid production in phytoplankton. *Glob. Change Biol.* **22**, 2744-2755.

Honaas, L. A., Wafula, E. K., Wickett, N. J., Der, J. P., Zhang, Y., Edger, P. P., Altman, N. S., Pires, J. C., Leebens-Mack, J. H. and dePamphilis, C. W. (2016).

Selecting superior de novo transcriptome assemblies: Lessons learned by leveraging the best plant genome. *PLoS ONE* **11**, e0146062.
Hove-Madsen, L. (1992). The influence of temperature on ryanodine sensitivity and the force-frequency relationship in the myocardium of rainbow trout. *J. Exp. Biol.* **167**, 47-60.
Hulbert, A. J. and Else, P. L. (2000). Mechanisms underlying the cost of living in animals. *Annu. Rev. Physiol.* **62**, 207-235.
Imbert-Auvray, N., Mercier, C., Huet, V. and Bois, P. (2013). Sarcoplasmic reticulum: a key factor in cardiac contractility of sea bass *Dicentrarchus labrax* and common sole *Solea solea* during thermal acclimations. *J. Comp. Physiol. B* **183**, 477-489.
IPCC (2013). Climate change 2013: The physical science basis. Contribution of working group I to the fifth assessment report of the Intergovernmental Panel on Climate Change (ed. T. F. Stocker, D. Qin, G.-K. Plattner, M. Tignor, S.K. Allen, J. Boschung, A. Nauels, Y. Xia, V. Bex and P.M. Midgley), pp. 1535.
Iwama, G. K. and Tautz, A. F. (1981). A simple growth model for salmonids in hatcheries. *Can. J. Fish. Aquat. Sci.* **38**, 649-656.
Kang, J. X. (2011). Omega-3: A link between global climate change and human health. *Biotechnol. Adv.* **29**, 388-390.
Kearse, M., Moir, R., Wilson, A., Stones-Havas, S., Cheung, M., Sturrock, S., Buxton, S., Cooper, A., Markowitz, S., Duran, C. et al. (2012). Geneious basic: an integrated and extendable desktop software platform for the organization and analysis of sequence data. *Bioinformatics* **28**, 1647-1649.
Keen, J. E., Vianzon, D.-M., Farrell, A. P. and Tibbits, G. F. (1994). Effect of temperature and temperature acclimation on the ryanodine sensitivity of the trout myocardium. *J. Comp. Physiol. B* **164**, 438-443.
Keen, A. N., Klaiman, J. M., Shiels, H. A. and Gillis, T. E. (2017). Temperature-induced cardiac remodelling in fish. *J. Exp. Biol.* **220**, 147-160.
Kraffe, E., Marty, Y. and Guderley, H. (2007). Changes in mitochondrial oxidative capacities during thermal acclimation of rainbow trout *Oncorhynchus mykiss*: roles of membrane proteins, phospholipids and their fatty acid compositions. *J. Exp. Biol.* **210**, 149-165.
Langmead, B. and Salzberg, S. L. (2012). Fast gapped-read alignment with Bowtie 2. *Nat. Methods* **9**, 357-359.
Lefrancois, C. and Claireaux, G. (2003). Influence of ambient oxygenation and temperature on metabolic scope and scope for heart rate in the common sole *Solea solea*. *Mar. Ecol. Prog. Ser.* **259**, 273-284.
Lopez-Jimena, B., Lyons, P., Herath, T., Richards, R. H., Leaver, M., Bell, J. G., Adams, A. and Thompson, K. D. (2015). The effect of dietary n-3/n-6 polyunsaturated fatty acid ratio on salmonid alphavirus subtype 1 (SAV-1) replication in tissues of experimentally infected rainbow trout (*Oncorhynchus mykiss*). *Vet. Microbiol.* **178**, 19-30.
Martin, N., Bureau, D. P., Marty, Y., Kraffe, E. and Guderley, H. (2012). Dietary lipid quality and mitochondrial membrane composition in trout: responses of membrane enzymes and oxidative capacities. *J. Comp. Physiol. B* **183**, 393-408.
Martinez, M. (2003). Condition, prolonged swimming performance and muscle metabolic capacities of cod *Gadus morhua*. *J. Exp. Biol.* **206**, 503-511.
Matikainen, N. and Vornanen, M. (1992). Effect of season and temperature acclimation on the function of crucian carp (*Carassius auratus*) heart. *J. Exp. Biol.* **167**, 203-220.
Mc Donald, D. G. and Milligan, C. L. (1992). 2 Chemical properties of the blood. In *Fish Physiology* (ed. W. S. Hoar, D. J. Randall and A. P. Farrell), pp. 55-133. Elsevier BV.
McKenzie, D. J. (2001). Effects of dietary fatty acids on the respiratory and cardiovascular physiology of fish. *Comp. Biochem. Physiol. A. Mol. Integr. Physiol.* **128**, 605-619.
McKenzie, D. J., Higgs, D. A., Dosanjh, B. S., Deacon, G. and Randall, D. J. (1998). Dietary fatty acid composition influences swimming performance in Atlantic salmon (*Salmo salar*) in seawater. *Fish Physiol. Biochem.* **19**, 111-122.
O'Neill, S. C., Perez, M. R., Hammond, K. E., Sheader, E. A. and Negretti, N. (2002). Direct and indirect modulation of rat cardiac sarcoplasmic reticulum function by *n*- 3 polyunsaturated fatty acids. *J. Physiol.* **538**, 179-184.
Owen, A. J., Peter-Przyborowska, B. A., Hoy, A. J. and McLennan, P. L. (2004). Dietary fish oil dose-and time-response effects on cardiac phospholipid fatty acid composition. *Lipids* **39**, 955-961.
Pahl, S. L., Lewis, D. M., Chen, F. and King, K. D. (2010). Heterotrophic growth and nutritional aspects of the diatom *Cyclotella cryptica* (Bacillariophyceae): effect of some environmental factors. *J. Biosci. Bioeng.* **109**, 235-239.
Patro, R., Duggal, G., Love, M. I., Irizarry, R. A. and Kingsford, C. (2017). Salmon provides fast and bias-aware quantification of transcript expression. *Nat. Methods* **14**, 417-419.
Person-Le Ruyet, J., Skalli, A., Dulau, B., Le Bayon, N., Le Delliou, H. and Robin, J. H. (2004). Does dietary n–3 highly unsaturated fatty acids level influence the European sea bass (*Dicentrachus labrax*) capacity to adapt to a high temperature? *Aquaculture* **242**, 571-588.
Pethybridge, H. R., Parrish, C. C., Morrongiello, J., Young, J. W., Farley, J. H., Gunasekera, R. M. and Nichols, P. D. (2015). Spatial patterns and temperature predictions of tuna fatty acids: Tracing essential nutrients and changes in primary producers. *PLoS ONE* **10**, e0131598.
Porter, R. K., Hulbert, A. J. and Brand, M. D. (1996). Allometry of mitochondrial proton leak: influence of membrane surface area and fatty acid composition. *Am. J. Physiol. Regul. Integr. Comp. Physiol.* **271**, R1550-R1560.
Quast, C., Pruesse, E., Yilmaz, P., Gerken, J., Schweer, T., Yarza, P., Peplies, J. and Glöckner, F. O. (2012). The SILVA ribosomal RNA gene database project: improved data processing and web-based tools. *Nucleic Acids Res.* **41**, D590-D596.
Raynard, R. S. and Cossins, A. R. (1991). Homeoviscous adaptation and thermal compensation of sodium pump of trout erythrocytes. *Am. J. Physiol.* **260**, R916-R924.
Rousseau, E., Smith, J. S. and Meissner, G. (1987). Ryanodine modifies conductance and gating behavior of single Ca^{2+} release channel. *Am. J. Physiol. Cell Physiol.* **253**, C364-C368.
Sargent, J. R., McEvoy, L. A. and Bell, J. G. (1997). Requirements, presentation and sources of polyunsaturated fatty acids in marine fish larval feeds. *Aquaculture* **155**, 117-127.
Schmieder, R. and Edwards, R. (2011). Fast identification and removal of sequence contamination from genomic and metagenomic datasets. *PLoS ONE* **6**, e17288.
Schurmann, H. and Steffensen, J. F. (1994). Spontaneous swimming activity of Atlantic cod *Gadus morhua* exposed to graded hypoxia at three temperatures. *J. Exp. Biol.* **197**, 129-142.
Shiels, H. A. and Farrell, A. (1997). The effect of temperature and adrenaline on the relative importance of the sarcoplasmic reticulum in contributing Ca^{2+} to force development in isolated ventricular trabeculae from rainbow trout. *J. Exp. Biol.* **200**, 1607-1621.
Shiels, H. A. and Farrell, A. P. (2000). The effect of ryanodine on isometric tension development in isolated ventricular trabeculae from Pacific mackerel (*Scomber japonicus*). *Comp. Biochem. Physiol. A. Mol. Integr. Physiol.* **125**, 331-341.
Shiels, H. A., Steven, E. D. and Farrell, A. P. (1998). Effects of temperature, adrenaline and ryanodine on power production in rainbow trout *Oncorhynchus mykiss* ventricular trabeculae. *J. Exp. Biol.* **201**, 2701-2710.
Shiels, H. A., Vornanen, M. and Farrell, A. P. (2002). The force–frequency relationship in fish hearts—a review. *Comp. Biochem. Physiol. A Mol. Integr. Physiol.* **132**, 811-826.
Shiels, H. A., Di Maio, A., Thompson, S. and Block, B. A. (2011). Warm fish with cold hearts: thermal plasticity of excitation–contraction coupling in bluefin tuna. *Proc. R. Soc. B Biol. Sci.* **278**, 18-27.
Simão, F. A., Waterhouse, R. M., Ioannidis, P., Kriventseva, E. V. and Zdobnov, E. M. (2015). BUSCO: assessing genome assembly and annotation completeness with single-copy orthologs. *Bioinformatics* **31**, 3210-3212.
Supek, F., Bošnjak, M., Škunca, N. and Šmuc, T. (2011). REVIGO summarizes and visualizes long lists of gene ontology terms. *PLoS ONE* **6**, e21800.
Swan, J. (2003). Effects of eicosapentaenoic acid on cardiac SR Ca^{2+}-release and ryanodine receptor function. *Cardiovasc. Res.* **60**, 337-346.
Thomassen, M. S. and Røsjø, C. (1989). Different fats in feed for salmon: influence on sensory parameters, growth rate and fatty acids in muscle and heart. *Aquaculture* **79**, 129-135.
Tocher, D. R. (2010). Fatty acid requirements in ontogeny of marine and freshwater fish. *Aquac. Res.* **41**, 717-732.
Turner, N., Else, P. L. and Hulbert, A. J. (2003). Docosahexaenoic acid (DHA) content of membranes determines molecular activity of the sodium pump: implications for disease states and metabolism. *Naturwissenschaften* **90**, 521-523.
Ushio, H., Ohshima, T., Koizumi, C., Visuthi, V., Kiron, V. and Watanabe, T. (1997). Effect of dietary fatty acids on Ca^{2+}-ATPase activity of the sarcoplasmic reticulum of rainbow trout skeletal muscle. *Comp. Biochem. Physiol. B Biochem. Mol. Biol.* **118**, 681-691.
Vagner, M., Zambonino Infante, J. L., Robin, J. H. and Person-Le Ruyet, J. (2007). Is it possible to influence European sea bass (*Dicentrarchus labrax*) juvenile metabolism by a nutritional conditioning during larval stage? *Aquaculture* **267**, 165-174.
Vagner, M., Lefrançois, C., Ferrari, R. S., Satta, A. and Domenici, P. (2008). The effect of acute hypoxia on swimming stamina at optimal swimming speed in flathead grey mullet *Mugil cephalus*. *Mar. Biol.* **155**, 183-190.
Vagner, M., Robin, J. H., Zambonino-Infante, J. L., Tocher, D. R. and Person-Le Ruyet, J. (2009). Ontogenic effects of early feeding of sea bass (*Dicentrarchus labrax*) larvae with a range of dietary n-3 highly unsaturated fatty acid levels on the functioning of polyunsaturated fatty acid desaturation pathways. *Br. J. Nutr.* **101**, 1452-1462.
Vagner, M., Zambonino-Infante, J.-L., Mazurais, D., Imbert-Auvray, N., Ouillon, N., Dubillot, E., Le Delliou, H., Akbar, D. and Lefrançois, C. (2014). Reduced n-3 highly unsaturated fatty acids dietary content expected with global change reduces the metabolic capacity of the golden grey mullet. *Mar. Biol.* **161**, 2547-2562.
Vagner, M., Lacoue-Labarthe, T., Zambonino Infante, J.-L., Mazurais, D., Dubillot, E., Le Delliou, H., Quazuguel, P. and Lefrançois, C. (2015). Depletion of essential fatty acids in the food source affects aerobic capacities of the golden grey mullet *Liza aurata* in a warming seawater context. *PLoS ONE* **10**, e0126489.
Vornanen, M. (1996). Effect of extracellular calcium on the contractility of warm-and cold-acclimated crucian carp heart. *J. Comp. Physiol. B* **165**, 507-517.
Vornanen, M. (1998). L-type Ca^{2+} current in fish cardiac myocytes: effects of thermal acclimation and beta-adrenergic stimulation. *J. Exp. Biol.* **201**, 533-547.

Vornanen, M., Shiels, H. A. and Farrell, A. P. (2002). Plasticity of excitation–contraction coupling in fish cardiac myocytes. *Comp. Biochem. Physiol. Part Mol. Integr. Physiol.* **132**, 827-846.

Vornanen, M., Hassinen, M., Koskinen, H. and Krasnov, A. (2005). Steady-state effects of temperature acclimation on the transcriptome of the rainbow trout heart. *Am. J. Physiol. Regul. Integr. Comp. Physiol.* **289**, R1177-R1184.

Wagner, G., Balfry, S., Higgs, D., Lall, S. and Farrell, A. (2004). Dietary fatty acid composition affects the repeat swimming performance of Atlantic salmon in seawater. *Comp. Biochem. Physiol. A. Mol. Integr. Physiol.* **137**, 567-576.

Waterhouse, R. M., Seppey, M., Simão, F. A., Manni, M., Ioannidis, P., Klioutchnikov, G., Kriventseva, E. V. and Zdobnov, E. M. (2018). BUSCO Applications from quality assessments to gene prediction and phylogenomics. *Mol. Biol. Evol.* **35**, 543-548.

Webb, P. W. (1975). Acceleration performance of rainbow trout (*Oncorhynchus mykiss*). *J Exp Biol* **63**, 451-465.

Wodtke, E. (1991). Temperature adaptation of biological membranes. Compensation of the molar activity of cytochrome C oxidase in the mitochondrial energy-transducing membrane during thermal acclimation of the carp (*Cyprinus carpio* L.). *Biochim. Biophys. Acta* **640**, 710-720.

Wu, F. C., Ting, Y. Y. and Chen, H. Y. (2003). Dietary docosahexaenoic acid is more optimal than eicosapentaenoic acid affecting the level of cellular defence responses of the juvenile grouper *Epinephelus malabaricus*. *Fish Shellfish Immunol.* **14**, 223-238.

Xiao, Y.-F., Gomez, A. M., Morgan, J. P., Lederer, W. J. and Leaf, A. (1997). Suppression of voltage-gated L-type Ca2+ currents by polyunsaturated fatty acids in adult and neonatal rat ventricular myocytes. *Proc. Natl. Acad. Sci. USA* **94**, 4182-4187.

Young, M. D., Wakefield, M. J., Smyth, G. K. and Oshlack, A. (2010). Gene ontology analysis for RNA-seq: accounting for selection bias. *Genome Biol.* **11**, R14.

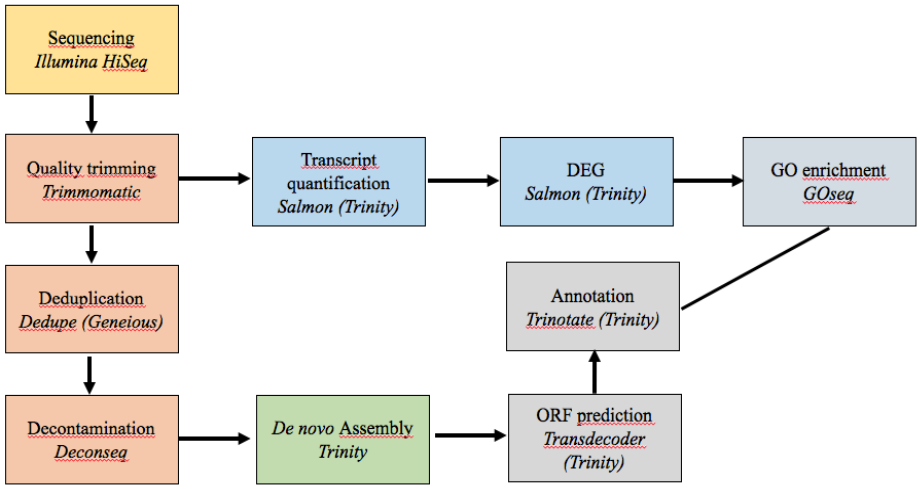

Figure S1. Transcriptomic analysis pipeline. This figure describes the steps performed in the transcriptomic analysis**.**

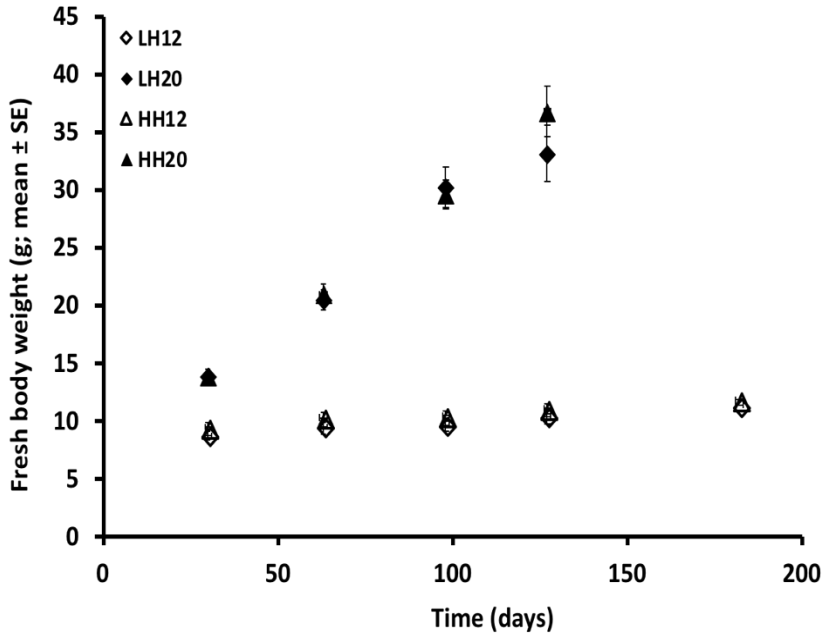

Figure S2. Growth curve of the four experimental groups of fish (HH12, LH12, HH20, LH20) tested and reared at 12°C or 20°C and fed the rich HUFA diet (HH) or the depleted HUFA diet (LH). The sample size was n = 34 (HH20), n = 20 (LH20), n = 37 (HH12) and n = 9 (LH12).

Table S1. Transcriptome assembly statistics. Assembly statistics based on the longest isoform per gene. The terminology corresponds to assembly with Trinity. BUSCO codes indicate the percentage of widely expressed genes that were recovered completely (C) (for single-copy (S) and duplicated (D) genes), that were only partially recovered (F for "Fragmented"), or that were missing (M). The total number of orthologous groups of genes (n) that was searched in BUSCO is also indicated.

Raw reads	661,022,788
Total assembled bases	123,209,874
Proportion of reads mapping back on the assembly (%)	92.1
Number of transcripts	328,877
Number of genes	189,77
Median contig length (bp)	349
Average contig length (bp)	649
Contig N50 (in bp, based on the longest isoform)	1474
BUSCO Eukaryota	C:95.7%[S:53.5%,D:42.2%],F:3.0%,M:1.3%,n:303
BUSCO Metazoa	C:95.0%[S:51.4%,D:43.6%],F:2.4%,M:2.6%,n:978
BUSCO Actinopterygii	C:74.4%[S:40.9%,D:33.5%],F:10.1%,M:15.5%,n:4584

Table S2. Summary table for GO terms summarised by REVIGO. Log10 FDR refers to the GO enrichment test performed by GOseq. Other headers are defined in Supek et al (2011).

Click here to Download Table S2

Table S3. Results of the GO enrichment analysis performed by GOseq within the Trinity pipeline (see methods). The four parts of the tables correspond to the four treatment comparisons conducted (HH12 vs. HH20, LH12 vs. LH20, HH12 vs. LH20, LH12 vs. HH20). Go terms are defined by the fields category, term (P for iological Process, for ellular omponent, F for olecular Function) and ontology (GO term description). numDEIn at and numIn at provide the number of transcript detected within each GO term, and whether they were detected as being differentially-expressed or not, respectively. gene ids provides the list of transcripts detected as differentially expressed. Significance of the enrichment tests are provided in the over represented pvalue and under represented pvalue, with their associated False Discovery Rate value (over represented FDR).

Click here to Download Table S3

Table S4 List of the unique 33 differentially-expressed transcripts from the enriched GO Terms involved in calcium-mediated processes, specific to the HH12-LH20 comparison (compared to HH12-HH20: Fig. 7 and Table 2). These GO terms are linked to the combined effect of elevated temperature and lowered concentration of HUFA in the diet and are involved in the following five biological processes: regulation of voltage-gated calcium channel activity (GO:1901385, 11 differentially-expressed transcripts), positive regulation of calcium-transporting ATPase activity (GO:1901896, 7 differentially-expressed transcripts), calcium ion trans-membrane transport via high voltage-gated calcium channel (GO:0061577, 4 differentially-expressed transcripts), regulation of cardiac muscle contraction by regulation of the release of sequestered calcium ion (GO:0010881, 16 differentially-expressed transcripts), and regulation of release of sequestered calcium ion into cytosol by sarcoplasmic reticulum (GO:0010880, 21 differentially-expressed transcripts). There are 59 differentially-expressed transcripts, 26 of which are involved in more than one GO term; we removed duplicates as to presenting the differentially-expression levels are Trinotate annotation results for the 33 transcripts involved in the set of five GO terms.

Click here to Download Table S4